

# Mechanisms of DNA Polymerases

Anthony J. Berdis\*

Department of Pharmacology, Case Western Reserve University, 10900 Euclid Avenue, Cleveland, Ohio 44106

Received November 23, 2008

## Contents

1. Introduction	2862
2. DNA Polymerization	2863
3. Chemical Mechanism of DNA Polymerization	2863
4. Kinetic Mechanism of DNA Polymerases	2864
4.1. Mechanism of Correct Nucleotide Incorporation	2865
4.2. Order of Substrate Addition	2865
4.3. Rate-Determining Steps Along the Reaction Pathway	2867
4.4. Kinetic Parameters for DNA Binding, Nucleotide Binding, and Polymerization	2868
4.5. Structural Perspectives on Nucleotide Incorporation	2869
4.6. Kinetic Steps After Phosphoryl Transfer	2870
4.7. Reversibility of DNA Polymerization	2870
5. Fidelity of Nucleotide Incorporation	2871
5.1. Forming a Mismatch: Alterations in the Kinetic Steps Associated with Polymerization	2871
6. Processing a Mismatch	2872
6.1. Role of Exonuclease Proofreading in Maintaining Genomic Fidelity	2872
6.2. Chemistry of Exonuclease Proofreading	2872
6.3. Kinetic Mechanism of Nucleotide Excision	2872
7. Polymerase Activity is Altered by DNA Damage	2873
7.1. Miscoding DNA Lesions	2873
7.2. Non-Instructional DNA Lesions	2873
7.3. Replication of Bulky DNA Lesions	2874
7.4. Thymine Dimers	2875
7.5. Replication of Cisplatin-Modified DNA	2875
8. Damage-Responsive DNA Polymerases	2876
8.1. Replication of Abasic Sites	2876
8.2. Damage-Responsive DNA Polymerase Replicate Bulky DNA Lesions with High Fidelity	2876
9. Therapeutic Interventions	2877
10. Conclusions	2877
11. References	2878



Dr. Anthony Berdis received his B.S. in Chemistry from Gannon University in Erie, Pennsylvania. He received his Ph.D. in Biochemistry from the University of North Texas in 1993. His graduate work, performed under the direction of Professor Paul F. Cook, focused on using steady-state kinetic approaches and heavy atom isotope effect measurements to elucidate the kinetic, chemical, and regulatory mechanisms of enzyme-catalyzed reactions. While in Texas, Dr. Berdis was a avid student of the martial arts (Muay Thai and Tae Kwon Do) and earned the nickname “Snake” in recognition for his fighting style. He then performed his NIH-sponsored postdoctoral fellowship under the direction of Professor Stephen J. Benkovic at The Pennsylvania State University. While in Professor Benkovic’s group, Dr. Berdis was fortunate to work on several projects ranging from the development of catalytic antibodies as novel biocatalysts to understanding multiprotein complexes involved in DNA replication. Dr. Berdis began his independent research career at Case Western Reserve University, where he continues to study the mechanism of DNA polymerases. His work focuses on developing non-natural natural nucleotides as chemical probes to study DNA polymerase activity on damaged DNA. His research has led to the development of new models invoking the importance of  $\pi$ -electron density as a predominant factor influencing polymerase fidelity during translesion DNA synthesis. In 2006, Dr. Berdis was presented the Henry W. Menn Memorial Award from the Skin Cancer Foundation recognizing his research towards understanding the mechanism of translesion DNA synthesis.

biological pathways that function in the oncogenic state versus the normal, healthy state. This knowledge is necessary to rationally design chemotherapeutic agents that selectively kill cancer cells while sparing their healthy counterparts.

It is well-established that a cancer cell is genetically different from its normal counterpart. Changes in genetic composition and context can occur by mutagenic events that are caused by inappropriate and/or dysfunctional DNA replication. In this review, we will explore the role that DNA polymerases play in cancer development and how their activities are exploited in various chemotherapeutic modalities. This will be accomplished by examining the mechanism for proper DNA synthesis and how defects in polymerase activity contribute to the initiation and progression of cancer.

At the cellular level, DNA polymerases catalyze the incorporation of mononucleotides into a growing primer

## 1. Introduction

The great Chinese strategist Sun Tsu wrote, “So it is said that if you know your enemies and know yourself, you will fight without danger in battles.”<sup>1</sup> This quote was originally meant to inspire warriors toward victory on a battlefield. Over two thousand years later, the same quote may be used to inspire scientists toward victory in the war on cancer. To win this war on cancer, we must completely understand the

\* E-mail: [ajb15@case.edu](mailto:ajb15@case.edu).

using a DNA template as a guide for directing each incorporation event. These enzymes perform the repetitive cycle of nucleotide binding, base-pairing, phosphodiester bond formation, product release, and movement to the next templating position at incredible rates with near-perfect accuracy. Perhaps the most remarkable feature of DNA polymerases is their ability to perform this cycle under the enormous strain of selecting the correct nucleotide substrate among four potential pairing partners. This chapter focuses on biochemical research performed over the past 20 years (1990 to the present) to provide insight into the mechanism by which DNA polymerases copy genomic DNA. The molecular events that underlie this process are understood by defining the rate and equilibrium constants for all the individual reactions involved in polymerization cycle that include binding of DNA and dNTP, conformational changes, phosphoryl transfer, and kinetic steps associated with product release. The dynamics of these various kinetic steps are discussed within the context of structural evidence for several different families of DNA polymerases in the absence and presence of DNA and nucleotide substrate. The molecular details for maintaining the fidelity of nucleotide incorporation are discussed with a particular emphasis on enzymatic activities that influence nucleotide incorporation and the kinetics of nucleotide removal by exonuclease proofreading activity. The influence of various DNA damaging agents on the mechanism and dynamics of DNA polymerization and exonuclease proofreading are discussed, focusing on their roles during cancer initiation and disease development. In addition, the ability of specialized, error-prone DNA polymerases to process replication blocks caused by DNA damaging agents is discussed. Finally, a brief description of anticancer agents targeting the activity of DNA polymerases is provided to highlight advances in chemotherapy. Collectively, this information provides the biochemical and biophysical basis for understanding replication fidelity and provides the framework for understanding how the efficiency and fidelity of DNA polymerases is altered by DNA damage to cause cancer.

## 2. DNA Polymerization

DNA is considered to be “the molecule of life” since it contains the genetic blueprint for all organisms ranging from simple viruses and bacteria to higher eukaryotes, including humans. The ability to accurately and efficiently duplicate DNA is essential for the survival and proliferation of any organism. The process of replicating an organism’s genomic material is complex and requires the coordinated efforts of an ensemble of proteins to initiate, propagate, and terminate each biochemical event in a timely and orderly fashion.<sup>2–4</sup> At the core of the replication process is the DNA polymerase, the enzyme that catalyzes the incorporation of mononucleotides into a growing polymer (primer) using a DNA template as a guide for directing each incorporation event. DNA polymerases are enigmatic enzymes as they maintain a remarkable degree of specificity despite the fact that the substrate requirement changes during each cycle of nucleotide incorporation due to the heteropolymeric nature of the genomic message. It is remarkable that the polymerase maintains an incredible degree of selectivity to insert only one of four potential deoxynucleoside 5′-triphosphates (dNTPs) opposite a template base while possessing an extraordinary degree of flexibility to recognize four distinct pairing partners (adenine:thymine, guanine:cytosine, thymine:

adenine, and cytosine:guanine). The polymerase performs the repetitive cycle of nucleotide binding, base-pairing, phosphodiester bond formation, product release, and movement to the next templating position at a rate of nearly 1000 bp/s.<sup>5</sup> An equally impressive feature is the incredible accuracy of this process. Replicative DNA polymerases have an error frequency of only 1 mistake for every 10<sup>6</sup> opportunities.<sup>6–8</sup> Collectively, the speed and accuracy of most DNA polymerases make them impressive catalysts. However, it is also recognized that defects in their overall efficiency can contribute significantly toward cancer initiation and progression.

## 3. Chemical Mechanism of DNA Polymerization

The overall reaction catalyzed by the vast majority of polymerases characterized to date is the template-directed incorporation of a dNTP into a growing primer stand in a 5′→3′ direction.<sup>9</sup> The chemistry required to elongate DNA is a simple phosphoryl transfer reaction<sup>10</sup> in which the  $\alpha$ -phosphate of the incoming dNTP undergoes nucleophilic attack by the 3′-OH of the primer strand of the nucleic acid (Figure 1). The reaction occurs in two distinct steps and is catalyzed with the participation of carboxylate residues that coordinate two metal ions (typically Mg<sup>2+</sup>) within the active site of the DNA polymerase. In this mechanism, an aspartate residue near the deoxyribose sugar of the incoming dNTP serves as the general base to abstract the proton from the 3′-OH to generate a more reactive nucleophile.<sup>11</sup> The electron-rich 3′-oxygen then attacks the  $\alpha$ -phosphate, creating a trigonal-bipyramidal pentacoordinated transition state that is stabilized through metal ion coordination with the oxygens of the  $\beta$ - $\gamma$  phosphate groups. This step results in the inversion of the  $\alpha$ -phosphate stereochemistry and the concerted release of the pyrophosphate leaving group coordinated to another divalent metal ion.

A similar two-step mechanism has been recently proposed by García-Díaz et al.<sup>12</sup> that is based upon structures of an error-prone DNA polymerase (human DNA polymerase  $\lambda$ ) in pre- and postcatalytic complexes. In addition, *ab initio* calculations reveal that significant charge transfer occurs during the reaction between both metals and various enzymatic residues within the active site and suggest that a concerted effort of metal ions and active site amino acids is required for efficient phosphoryl transfer.<sup>13</sup>

Detailed information regarding the nature of the transition state of the phosphoryl transfer reaction has been provided by studies evaluating leaving group effects on the polymerization reaction.<sup>14</sup> These studies monitored the incorporation of dNTP analogues in which the  $\beta,\gamma$ -bridging oxygen is replaced with CH<sub>2</sub>, CHF, CF<sub>2</sub>, or CCl<sub>2</sub>.<sup>14</sup> Kinetic analyses reveal that all analogues are incorporated opposite correct and incorrect pairing partners with fidelity factors similar to natural dNTPs.<sup>14</sup> More importantly, however, is the fact that the rate constants for incorporation vary as a function of the modified  $\beta,\gamma$ -bridging group.<sup>14</sup> Bronsted correlations determined from the log of the rate constant for incorporation versus leaving group pK<sub>a</sub> for correct and incorrect incorporation reveal similar sensitivities followed by departures from linearity.<sup>14</sup> These analyses suggest that phosphoryl transfer is the rate-limiting step for the correct and incorrect nucleotide incorporation for polymerase beta. Although it is unlikely that this conclusion is universal for all DNA polymerases, these data are important because they indicate

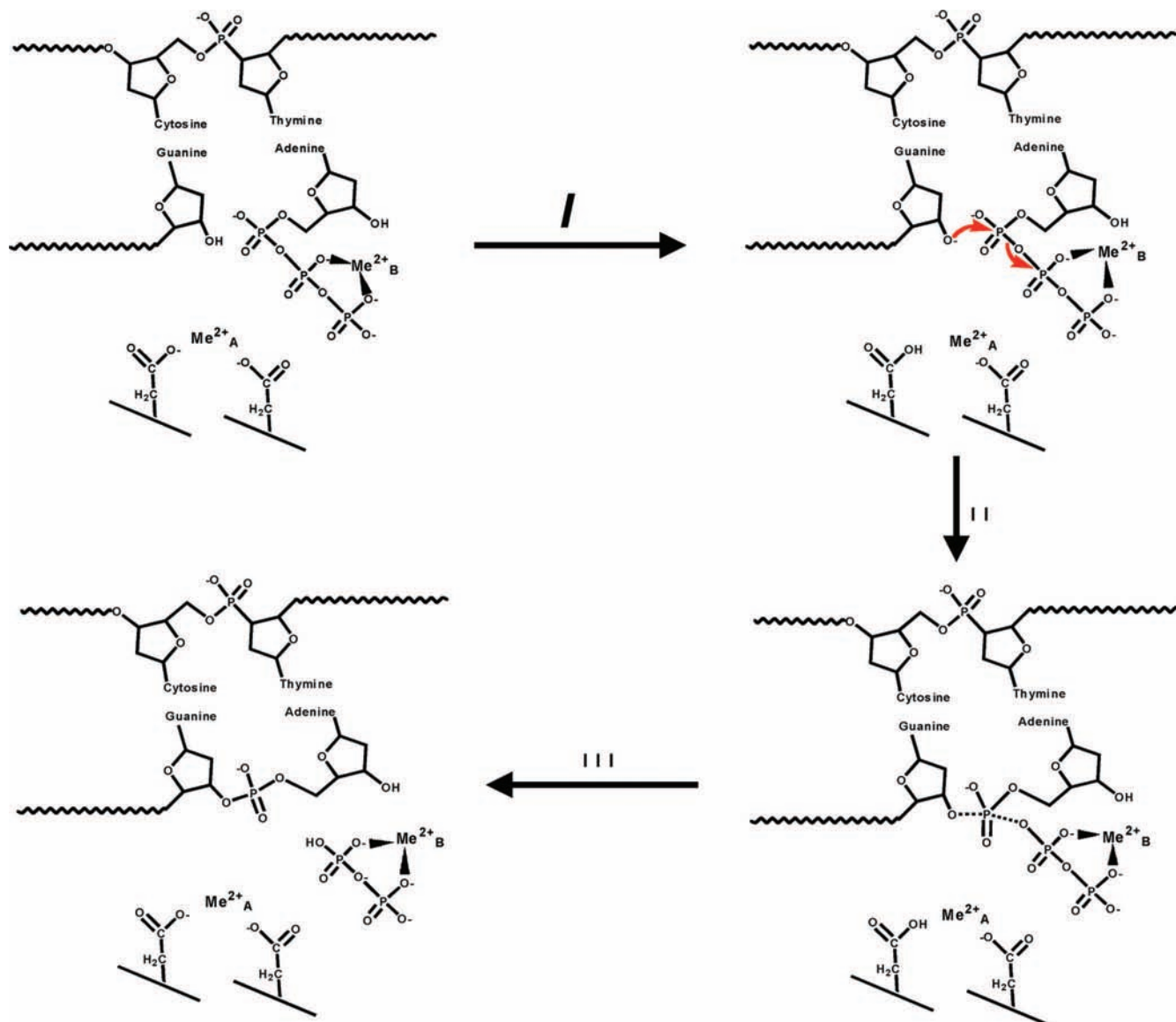


**Figure 1.** Chemical mechanism for phosphoryl transfer catalyzed by DNA polymerases. In this mechanism, an aspartate residue near the deoxyribose sugar of the incoming dNTP serves as the general base to abstract the proton from the 3'-OH to generate a more reactive nucleophile. The electron-rich 3'-oxygen then attacks the  $\alpha$ -phosphate, creating a trigonal-bipyramidal pentacoordinated transition state. The release of the pyrophosphate leaving group occurs via coordination to another divalent metal ion.

how the attainment of the proper transition state can influence polymerization fidelity.

#### 4. Kinetic Mechanism of DNA Polymerases

DNA polymerases perform this simple phosphoryl transfer reaction under the enormous strain of selecting the correct nucleotide substrate among four potential pairing partners. This ability has historically been attributed to hydrogen-bonding interactions that are often used to explain how each incorporation event occurs efficiently and selectively. Figure 2 shows the hydrogen bonding scheme for T:A and C:G base pairs, respectively. At the atomic level, the NH groups of the bases are good hydrogen bond donors (denoted as *d*) while the electron pairs on the oxygens of C=O groups and on the ring nitrogens are hydrogen bond acceptors (denoted as *a*). The hydrogen bonding capability of an T:A base pair uses complementarity of *d-a(-)* to *a-d-a*, while the C:G base pair uses complementarity of *a-d-d* to *d-a-a*. In planar base pairs, the hydrogen bonding pattern yields a geometry that gives an interglycosyl distance (C-1' to C-1') of 10.60  $\pm$

0.40  $\text{\AA}$  and an angle of  $55 \pm 2^\circ$  between the glycosylic bonds for both the T:A and C:G base pairs. The geometry afforded by these parameters indicates that all four base pair combinations—A:T, T:A, G:C, and C:G—can exist within the regular framework of duplex DNA.

Unfortunately, the groups that provide favorable hydrogen bonding interactions are highly reactive and, thus, susceptible to modifications that can influence the mechanism and fidelity of DNA polymerases. As illustrated in Figure 3, simple alkylating agents such as methyl methane sulfonate (MMS) and *N*-methyl-*N*'-nitro-*N*-nitrosoguanidine (MNNG) preferentially react with the N3 and N7 positions of adenine and the O6 and N7 position of guanine.<sup>15–17</sup> Alkylation at the O6 position of guanine changes both the hydrogen bonding capabilities and tautomeric form of guanine, which increases the frequency of misincorporation events. In addition, alkylating agents can create abasic sites by enhancing the hydrolysis of *N*-glycosidic bond that occurs nonenzymatically<sup>18,19</sup> or via the action of various DNA glycosylases.<sup>20–22</sup> Later sections will describe how inappropriate alterations to the

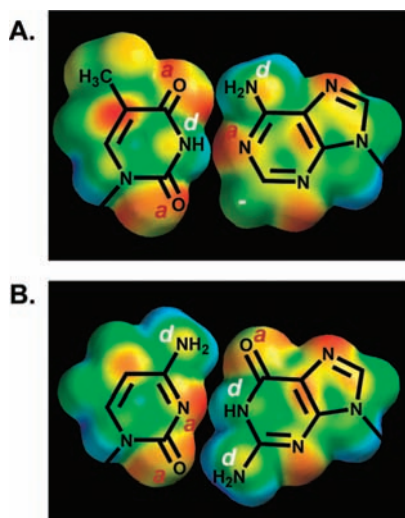


**Figure 2.** Hydrogen bonding interactions between Watson–Crick base pairs (A) thymine:adenine and (B) cytosine:guanine. Hydrogen bond donors are denoted as *d*, while hydrogen bond acceptors are denoted as *a*. Using this scheme, the hydrogen bonding capability of a T:A base pair uses complementarity of *a-d-a* to *d-a(-)* while the C:G base pair uses complementarity of *d-a-a* to *a-d-d*.

hydrogen bonding potential of a templating base can lead to mutagenesis and induce carcinogenesis.

#### 4.1. Mechanism of Correct Nucleotide Incorporation

To define the mechanism of correct nucleotide incorporation by any DNA polymerase, it is necessary to first understand the rate and equilibrium constants for all individual reactions involved in DNA synthesis. Data from a series of kinetic,<sup>23–29</sup> mutational,<sup>30–33</sup> and structural<sup>34–43</sup> studies have been collectively used to describe DNA polymerization via the multiplicative mechanism outlined in Figure 4. This is an ordered kinetic mechanism in which the DNA polymerase binds DNA substrate prior to the binding of dNTP. The first point for generating catalytic efficiency and maintaining fidelity occurs during the binding of dNTP to the polymerase:DNA complex (Step 2). After dNTP binding, a conformational change (Step 3) in the polymerase and nucleic acid is proposed to align the incoming dNTP into a precise geometrical conformation that allows for phosphoryl transfer (Step 4). The involvement of the conformational change is consistent with a proposed “induced-fit” mechanism that imposes discrimination against dNTP misincorporation since misaligned intermediates disrupt the geometry of the polymerase’s active site to hinder the chemical step.<sup>28</sup>

After the nucleotide is covalently added to the growing primer, there is a conformational change step in the polymerase that relaxes the E':DNA<sub>*n+1*</sub>:PP<sub>*i*</sub> to the E:DNA<sub>*n+1*</sub>:PP<sub>*i*</sub> species (Step 5). Following this step, the first product, PP<sub>*i*</sub>, is released from the polymerase (Step 6) upon which the enzyme presumably translocates to the next templating position. At this point, the polymerase can remain bound to the product DNA (DNA<sub>*n+1*</sub>) to continue synthesis on the same nucleic acid substrate (Step 7) or dissociate from the DNA<sub>*n+1*</sub> to renew polymerization on another substrate (Step 8).

The following sections describe key experiments employing steady-state and presteady-state kinetic approaches to validate the mechanism of this DNA polymerization pathway.

These techniques have been reviewed elsewhere<sup>45,46</sup> and the reader is referred to these sources for further details. Briefly, steady-state kinetic measurements are performed in which the concentration of DNA and dNTP substrates is maintained in molar excess versus the concentration of DNA polymerase. This approach has several important advantages. First, these experiments require relatively low amounts of polymerase and do not require specialized equipment to obtain data. Furthermore, steady-state techniques have proven useful in determining the order of substrate binding and product release as well as giving information regarding the location of the rate-limiting step(s) during nucleotide incorporation and enzyme turnover. Unfortunately, steady-state methods are limited in their inability to directly measure dissociation and kinetic rate constants that precede and/or follow the rate-limiting step of the reaction.<sup>44</sup> As a result, presteady-state methods capable of examining the polymerization reaction on a millisecond time scale are used to provide this information. One advantage is the ability to monitor for bursts in polymerization products that occur upon mixing polymerase and substrates under pseudofirst-order conditions (DNA in excess of enzyme). Experiments can also be performed using single turnover conditions in which the concentration of polymerase is maintained in excess versus DNA substrate. This condition allows kinetic steps associated with initial product formation to be accurately measured since complications caused by the involvement of potential rate-limiting steps that occur after phosphoryl transfer are avoided. Major disadvantages of employing presteady-state techniques include the use of higher concentrations of polymerase and DNA substrate as well as the requirement for specialized equipment<sup>46</sup> to monitor the reaction on a short time scale (millisecond to seconds).

#### 4.2. Order of Substrate Addition

Theoretically, the binding of DNA and dNTP substrates to the polymerase can be random, sequential, or strictly ordered. However, efficient polymerization would be optimal through the strictly ordered binding of DNA substrate prior to dNTP, since the converse order of substrate addition (initial binding of dNTP prior to DNA) would be correct only once out of four opportunities. High-fidelity polymerases involved in chromosomal DNA synthesis are expected to display an obligatory order of substrate addition of binding DNA prior to nucleotide. However, a different scenario could be used by error-prone DNA polymerases that are involved in replicating damaged DNA. In this instance, the order of substrate addition becomes important since error-prone DNA polymerases generally incorporate a single nucleotide without using “correct” templating information. As a result, error-prone polymerases could bind dNTP substrate prior to interacting with damaged DNA.

The order by which high-fidelity polymerases bind DNA and dNTP is generally assessed by one of three general methods. Early work focused on steady-state inhibition studies by PP<sub>*i*</sub> to deduce the overall kinetic mechanism of polymerization.<sup>23</sup> Inhibition by PP<sub>*i*</sub> at varying dNTP concentrations gave a series of parallel lines on a double reciprocal plot, indicative of uncompetitive inhibition. In contrast, inhibition by PP<sub>*i*</sub> at different concentrations of DNA yielded a mixed inhibition pattern, suggesting that PP<sub>*i*</sub> forms a dead-end complex with the E:DNA<sub>*n*</sub> species or noncompetitively inhibits the E:DNA:dNTP complex. The collective PP<sub>*i*</sub> inhibition patterns were consistent with an ordered

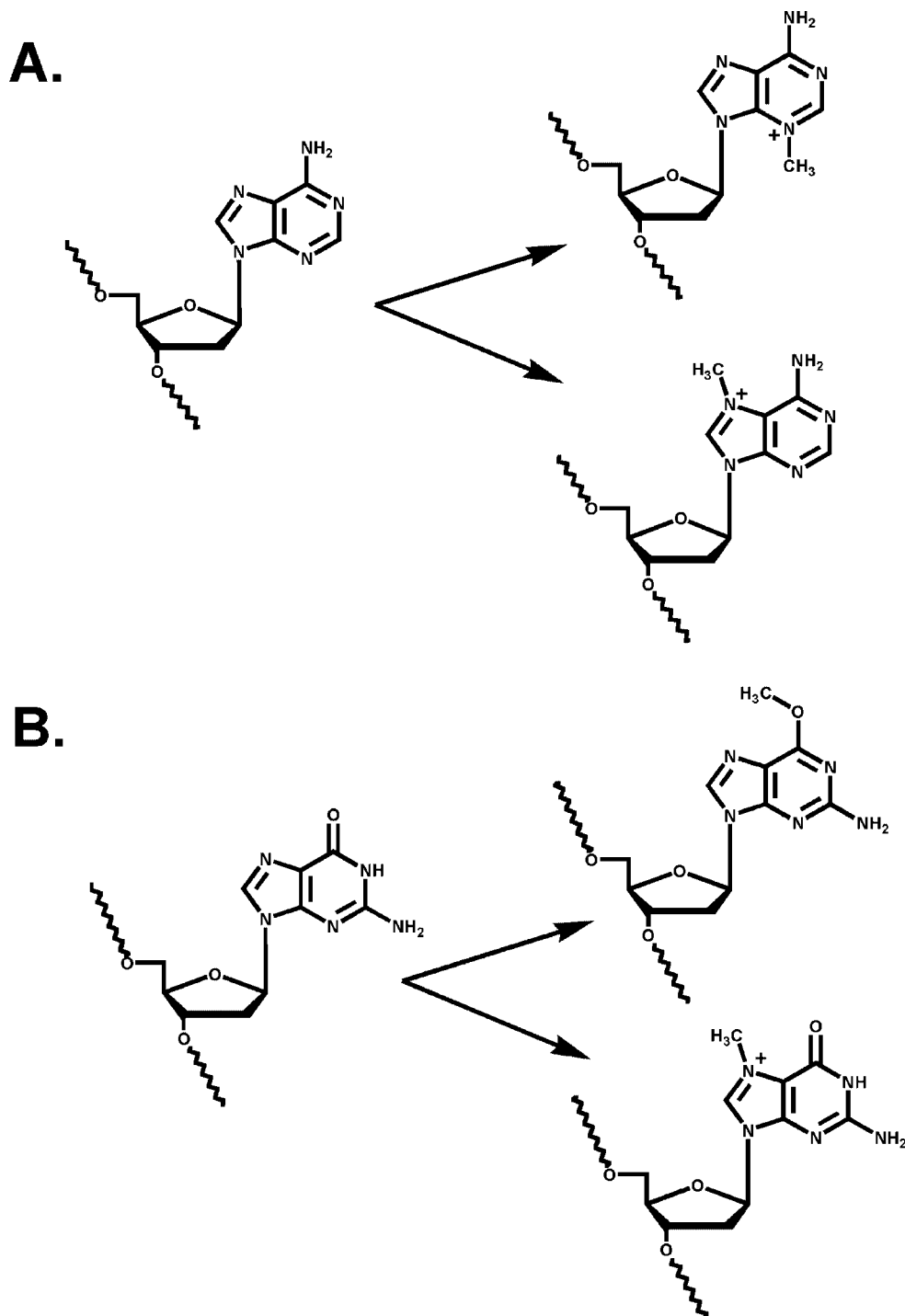


**Figure 3.** Nonenzymatic modifications to (A) adenine and (B) guanine. See text for further discussions.

sequential binding mechanism in which the polymerase binds to DNA prior to dNTP.

The second method for determining the order of binding is the use of isotope trapping techniques.<sup>24</sup> In these experiments, the polymerase was first incubated with labeled dNTP followed by the addition of DNA and a large excess of unlabeled dNTP substrate to initiate the reaction. The lack of product formation measured under these conditions indicates that any bound dNTP substrate is either diluted into the unlabeled pool via dissociation or, more likely, that DNA must bind prior to dNTP. This latter conclusion can be confirmed by demonstrating product formation under conditions in which the polymerase is incubated with labeled DNA

followed by initiation of the addition of dNTP and a large excess of unlabeled DNA substrate.

Finally, the order of substrate binding can be independently confirmed by measuring the processivity of the polymerase. Processivity is defined as the number of nucleotides incorporated by a polymerase during a single binding event to a DNA substrate. Values for processivity range from 1 for a completely distributive enzyme to hundreds or thousands of nucleotide incorporation events for more processive polymerases. One approach to evaluate polymerase processivity is a template challenge experiment that employs two different DNA substrates. Early experiments simply added an excess of poly(dC)\*oligo (dG) and dGTP to a reaction in which

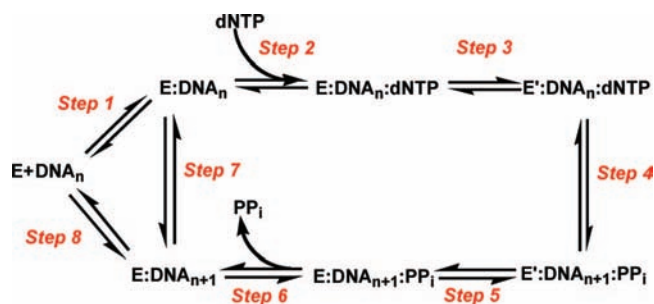


**Figure 4.** Kinetic mechanism for most DNA polymerases. Step 1 is the binding of polymerase (E) to DNA substrate. Step 2 involves dNTP binding to the polymerase/DNA complex. Step 3 represents a conformational change in the polymerase:DNA complex that is followed by phosphoryl transfer (Step 4). After the nucleotide is covalently added to the growing primer, there is a conformational change step in the polymerase that relaxes the  $E':DNA_{n+1}:PP_i$  to the  $E:DNA_{n+1}:PP_i$  species (Step 5). Following this step,  $PP_i$  is released as the first product from the polymerase (Step 6). At this stage, the polymerase can remain bound to the product DNA ( $DNA_{n+1}$ ) to continue synthesis on the same nucleic acid substrate (Step 7) or dissociate from the  $DNA_{n+1}$  to renew polymerization on another substrate (Step 8).

the polymerase was actively replicating a poly(dA)\*oligo(dT) substrate.<sup>25</sup> The length of time required for the cessation of dTTP incorporation provides a measure of polymerase processivity. An alternative method is a pulse-chase experiment in which the polymerase is first incubated with labeled DNA followed by the sequential addition of dNTP to initiate the reaction and a large excess of unlabeled DNA to “chase” any polymerase that has dissociated from the labeled DNA substrate. The number of nucleotides added to the labeled DNA after the addition of the “chase” provides a direct indication of polymerase processivity. In general, polymerases such as the bacteriophage T4 DNA polymerases<sup>47</sup> and the eukaryotic pol  $\delta$ <sup>48</sup> that are involved in chromosomal replication have high processivity factors of >100 that are significantly increased by association with various accessory factors.<sup>49,50</sup> In contrast, polymerases involved in specialized functions such as DNA repair (Klenow fragment and pol  $\beta$ ) or lesion bypass (pol  $\eta$ , pol  $\iota$ , pol  $\zeta$ ) have low processivity factors of 10 or less and are, thus, more distributive in nature.<sup>51–56</sup>

### 4.3. Rate-Determining Steps Along the Reaction Pathway

The rate-limiting step for polymerization could be the phosphoryl transfer step or physical steps flanking either side of this chemistry step that include substrate association, conformational changes, or steps associated with product release. Again, steady-state experiments were instrumental in providing evidence that a step after phosphoryl transfer is rate-limiting for polymerase turnover. In these experiments, extrapolation of the time course in product formation back to zero time showed an intercept above the y-axis rather than through the origin.<sup>26</sup> This time course is indicative of “burst” or biphasic kinetics. Biphasic kinetic behavior could reflect heterogeneity in enzyme and/or substrate or, more likely, the participation of more than one kinetic event in the observed rate in product formation. Indeed, quantitative analyses indicated that the bursts in product formation were proportional to the concentration of polymerase used in the reaction and provided evidence for a reaction mechanism

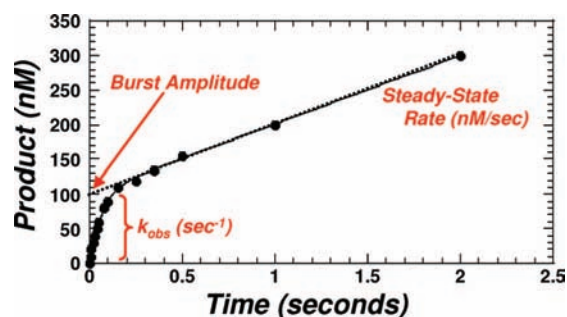


**Figure 5.** Biphasic time course in nucleotide incorporation catalyzed by most replicative DNA polymerases in a reaction performed using DNA and dNTP substrate in excess of polymerase. In general, the burst amplitude reflects the concentration of active enzyme. The observed rate constant for the burst phase ( $k_{obs}$ ) defines the rate constant for the first nucleotide incorporation event. The state-steady rate defines the overall rate of product formation for multiple enzyme turnovers and reflects the rate-limiting step of the polymerization reaction.

with rapid initial dNTP incorporation followed by a slower rate that is rate-limiting in the steady state.

However, precise quantification of the burst rate and amplitude in product formation required the utilization of presteady-state kinetic techniques. Excellent reviews on rapid chemical-quench and stopped-flow spectroscopic techniques used in these studies can be found elsewhere.<sup>57,58</sup> The primary advantage of using presteady-state techniques is the ability to monitor the reaction on a millisecond time scale.<sup>57</sup> Figure 5 illustrates a typical biphasic time course for nucleotide incorporation in a polymerization reaction performed while maintaining the concentration of DNA and dNTP substrate in excess of polymerase. The data can be fit to the equation defining a single exponential followed by a linear function ( $y = A e^{-k_{obs}t} + Bt + C$ ). The amplitude of the fast “burst” phase is stoichiometric with the amount of polymerase present in the reaction.<sup>59</sup> The  $k_{obs}$  defines the first-order rate constant for the fast phase. This value is independent of polymerase concentration but dependent on dNTP concentration (vide supra). The second, slower phase reflects the steady-state rate of dNTP incorporation and, in contrast to the first phase, is dependent on polymerase concentration but independent of dNTP concentration. Reducing the concentration of dNTP decreases the rate constant of the fast phase but not the rate of the slow phase. This behavior indicates that the polymerization mechanism involves an initial rapid step followed by a slower, first-order process. This is indicative of rapid incorporation of one dNTP per enzyme-bound molecule followed by a slow dissociation of product DNA, which is rate-limiting for polymerase turnover. Using the *E. coli* Klenow fragment as a model,<sup>27</sup> the  $k_{pol}$  value for the “burst phase” is  $50 \text{ s}^{-1}$  while the rate constant for polymerase turnover ( $k_{cat}$ ) is significantly slower at  $\sim 0.1 \text{ s}^{-1}$ . With the bacteriophage T4 and T7 DNA polymerase systems,  $k_{pol}$  values range from  $100\text{--}250 \text{ s}^{-1}$  while the  $k_{cat}$  value is approximately 50-fold slower at  $\sim 2 \text{ s}^{-1}$ .<sup>28,29</sup> In all cases, the differences between rate constants in initial nucleotide incorporation and enzyme turnover clearly indicate that a kinetic step after phosphoryl transfer such as product release is rate-limiting for enzyme turnover.

If product release is the rate-limiting step for polymerase turnover, then what limits the rate for the incorporation of the first nucleotide? The answer to this question is important because it provides essential information regarding how kinetic step(s) such as nucleotide binding, conformational

changes, and/or phosphoryl transfer participate in regulating fidelity. One of the earliest (and arguably most controversial) probes used to evaluate the location of the rate-limiting step has been the application of thio-substituted nucleotides on the rate of nucleotide incorporation. Because of decreased electronegativity, a nonbridging sulfur atom is predicted to be less effective than oxygen at stabilizing electron density for an associative transition state during a phosphoryl transfer reaction. As such, one can measure the magnitude of a “thio effect” (rate with  $\alpha$ -O-dNTP divided by the rate with  $\alpha$ -S-dNTP) as a diagnostic indication of whether chemistry is rate-limiting. If chemistry is the rate-limiting step, then a large thio-elemental effect ( $>10$ ) will be observed. In contrast, a small thio-elemental effect of  $<2$  will be observed if another kinetic step such as a conformational change preceding phosphoryl transfer is rate-limiting and insensitive to this type of substitution.

In the case of the *E. coli* Klenow fragment and the bacteriophage T4 DNA polymerase, substitution of an  $\alpha$ -S-dNTP for the corresponding  $\alpha$ -O-dNTP led to a slight decrease ( $<2$ ) in the rate constant of the fast, burst phase.<sup>27</sup> The minimal reduction upon this substitution suggests that chemical bond formation during the phosphoryl transfer step does not limit the incorporation of the first nucleotide. Further support for this mechanism is derived from a series of spectroscopic studies monitoring the enzymatic incorporation of dTTP opposite 2-aminopurine (2-AP) present in the template strand.<sup>60</sup> 2-AP is a highly fluorescent constitutional analogue of adenine. The fluorescence of 2-AP is strongly quenched via hydrogen bonding and base-stacking interactions.<sup>61</sup> As a result, the incorporation of a dNTP opposite 2-AP can be easily monitored via a change in fluorescence caused by nucleotide incorporation and compared to rates obtained using conventional radiolabeled assays. Indeed, the kinetics of dTTP incorporation opposite 2-AP were initially evaluated by Frey et al.<sup>60</sup> using the *E. coli* Klenow fragment and bacteriophage T4 DNA polymerases as models. Their studies with the Klenow fragment demonstrated an identical rate constant of  $7 \text{ s}^{-1}$  for dTTP incorporation opposite 2-AP using either rapid-quenching techniques or stopped-flow fluorescence methods.<sup>60</sup> The identity in rate constants using either assay suggests that the quenching of 2-AP is associated with the conformational change step that precedes phosphoryl transfer. Similar results were obtained using the bacteriophage T4 DNA polymerase.<sup>60</sup> Collectively, the data indicate that the rate constant for the fast phase of nucleotide incorporation reflects a rate-limiting conformational change of the E:DNA<sub>n</sub>:dNTP complex to E':DNA:dNTP that precedes chemical bond formation.

It should be noted that there is significant debate regarding if the conformational change step preceding phosphoryl transfer is rate-limiting for all DNA polymerases. This controversy involves using the magnitude of a thio-elemental effect to unambiguously define the rate-limiting step for nucleotide incorporation.<sup>62,63</sup> For example, Showalter and Tsai<sup>63</sup> argue that thio-elemental effects are unreliable because the effect on the enzyme-catalyzed phosphoryl transfer reaction is assumed to be identical to that on the uncatalyzed reaction. However, this assumption cannot be made if the molecular details of the transition state for the enzymatic reaction are not accurately defined. Furthermore, it is argued that the uncatalyzed phosphoryl transfer reaction occurs in an achiral environment in which all nonbridging oxygens make an equal inductive contribution toward stabilizing an

associative transition state.<sup>63</sup> The same conclusion is unlikely for the enzyme-catalyzed reaction since metal ion coordination occurs exclusively with one nonbridging oxygen and would generate a lower thio-effect for the enzyme-catalyzed reaction.<sup>63</sup>

Additional arguments are supplied by spectroscopic studies monitoring nucleotide incorporation by pol  $\beta$ .<sup>64</sup> Stopped-flow fluorescence studies of correct nucleotide incorporation reveal two fluorescence transitions that occur prior to and after the chemical step.<sup>64</sup> Surprisingly, the rate constant for the fluorescence transition that occurs prior to phosphoryl transfer is at least 5 times faster than the rate constant for nucleotide incorporation. As described earlier, Bronsted correlations determined from the log of the rate constant for incorporation versus leaving group pK<sub>a</sub> for nucleotide incorporation also suggest that phosphoryl transfer is rate-limiting for pol  $\beta$ .<sup>14</sup> Collectively, these data argue that, for pol  $\beta$ , the rate-limiting step for nucleotide incorporation is phosphoryl transfer and not a conformational change step. It is not clear whether other DNA polymerases show similar kinetic behavior. However, this information indicates that, while polymerases catalyze the same chemical reaction, they employ different strategies to achieve rate enhancements and fidelity during nucleotide incorporation. More detailed kinetic studies are needed to evaluate the nature of the rate-limiting step for other DNA polymerases, especially with respect to error-prone polymerases that are involved in processing damaged DNA.

#### 4.4. Kinetic Parameters for DNA Binding, Nucleotide Binding, and Polymerization

A variety of kinetic techniques have been used to measure the binding affinity of DNA substrates to various DNA polymerases. Early attempts using steady-state approaches measured turnover rates at various concentrations of DNA. The linear time courses were extrapolated back to time zero and revealed a burst in primer elongation that was equivalent to the amount of E:DNA complex present prior to initiating the reaction.<sup>27</sup> Presteady-state techniques have also measured the burst amplitudes and rate constants for nucleotide incorporation.<sup>28</sup> In either case, the  $K_d$  for DNA substrate is obtained using the quadratic equation:  $[E:DNA] = 0.5(K_d + [E] + [DNA] - 0.25(K_d + [E] + [DNA])^2 - [E:DNA])^{1/2}$ , where  $[E]$  is the concentration of T4 DNA polymerase,  $[DNA]$  is the concentration of nucleic acid, E:DNA is the burst amplitude, and  $K_d$  is the dissociation binding constant for DNA. With the bacteriophage T4 DNA polymerase, the binding affinity for DNA ( $K_{d \text{ DNA}}$ ) is high at 10 nM and relatively independent of sequence context.<sup>28,29</sup> The association rate constant,  $k_{\text{on}}$ , for DNA binding to polymerase is calculated from the relationship  $K_d = k_{\text{off}}/k_{\text{on}}$ . Using the bacteriophage T4 DNA polymerase as an example, a  $k_{\text{on}}$  value of  $\sim 10^7 \text{ M}^{-1} \text{ s}^{-1}$  is calculated using a  $K_d$  of 10 nM and a  $k_{\text{off}}$  value of  $2 \text{ s}^{-1}$ .

A similar approach can be used to empirically measure the binding affinity ( $K_{d \text{ dNTP}}$ ) for nucleotide substrate and the maximal rate constant of polymerization,  $k_{\text{pol}}$ . In these experiments, the rate constant of the burst phase ( $k_{\text{obs}}$ ) is measured as a function of variable dNTP concentration (Figure 6A). Plotting the data as  $k_{\text{obs}}$  versus dNTP concentration (Figure 6B) is a rectangular hyperbola that, when fit to the Michaelis–Menten equation ( $k_{\text{obs}} = k_{\text{pol}}[\text{dNTP}]/(K_d + [\text{dNTP}])$ ), defines the kinetic parameters  $K_d$ ,  $k_{\text{pol}}$ , and  $k_{\text{pol}}/K_d$ . For most DNA polymerases, the  $K_d$  value for the incorporation of a dNTP opposite its Watson–Crick partner

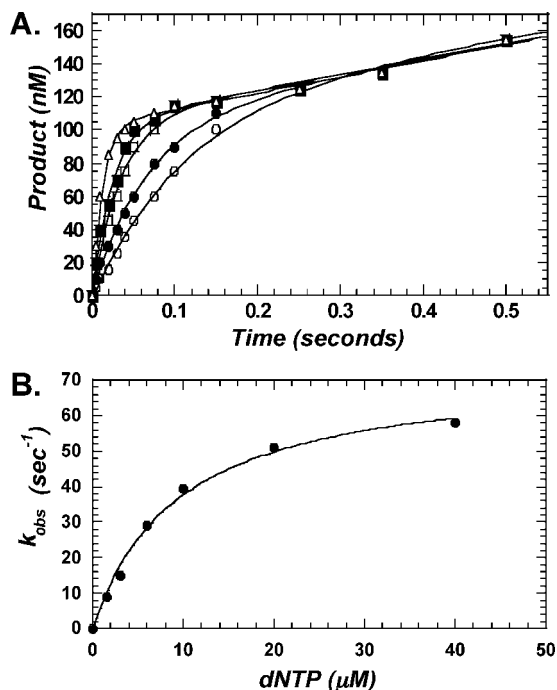


**Figure 6.** Representative data analyses used to measure the kinetic parameters for nucleotide incorporation,  $K_d$  dNTP and  $k_{pol}$ . (A) The rate constant of the burst phase ( $k_{obs}$ ) varies as a function of dNTP concentration. However, the burst amplitude and steady-state rate for nucleotide incorporation remain independent of dNTP concentration. (B) A plot of the data as  $k_{obs}$  versus dNTP concentration yields a rectangular hyperbola that, when fit to the Michaelis–Menten equation ( $k_{obs} = k_{pol}[dNTP]/(K_d + [dNTP])$ ), provides the kinetic parameters  $K_d$ ,  $k_{pol}$ , and  $k_{pol}/K_d$ .

is  $\sim 10 \mu\text{M}$ .<sup>65</sup> For replicative DNA polymerases,  $k_{pol}$  values for the incorporation of a dNTP opposite its Watson–Crick partner generally range from 25–400 s<sup>-1</sup>. Thus, the overall catalytic efficiency ( $k_{pol}/K_d$ ) for enzymatically forming a Watson–Crick base pair is  $\sim 10^7 \text{ M}^{-1} \text{ s}^{-1}$ , a value that places DNA polymerases in the upper hierarchy of most proficient enzymes.

#### 4.5. Structural Perspectives on Nucleotide Incorporation

Kinetic characterization of the enzymatic reaction provides the basic framework for understanding the mechanism of correct DNA polymerization. However, the dynamics of the various kinetic steps have been elucidated by solving the structures of various DNA polymerases in the absence and presence of DNA and nucleotide substrate. The most extensively characterized families of DNA polymerases are the A and B families, which include the Klenow fragments of DNA polymerase I from *Escherichia coli*<sup>35–37</sup> and *Bacillus subtilis*,<sup>38–40</sup> *Thermus aquaticus* DNA polymerase,<sup>41</sup> the bacteriophage T7 DNA polymerase,<sup>42,43</sup> and the bacteriophage RB69 DNA polymerase.<sup>66–69</sup> The model provided in Figure 7 shows that DNA polymerases possess a common structural architecture resembling a “right hand” containing fingers, palm, and thumb subdomains.<sup>70</sup> The palm domain is the most closely conserved structural feature because it is responsible for catalyzing the phosphoryl transfer reaction. The palm domain contains at least two carboxylic acid amino acids (aspartate and/or glutamate) that function to coordinate the two catalytically essential metal ions that participate in phosphoryl transfer. The fingers domain interacts with the incoming dNTP as well as the templating base and thus plays

an important role in maintaining fidelity. The thumb domain plays dual roles by positioning duplex DNA for the incoming dNTP as well as in the processivity and translocation of the polymerase. Models correlating structural movements with kinetic phenomenon suggest that dNTP binds to the polymerase:DNA complex in a template-independent manner first by interacting with the fingers domain. This initial binding event is followed by a rotation of the fingers domain that induces “tighter” binding with the templating nucleobase and reflects the conformational change step. This is illustrated in Figure 7 showing the model of the KlenTaq polymerase in an “open” conformation (Figure 7A) going to a “closed” conformation (Figure 7B) due to rotation of the fingers domain.<sup>71</sup> This rotation is proposed to provide the driving force required to align the incoming dNTP with its complementary partner as well as to orient the 3′-hydroxyl of the primer for attack on the bound dNTP. Similar open and closed conformations have been observed in error-prone (X-family) DNA polymerases,<sup>72,73</sup> B-family polymerases,<sup>74–78</sup> and HIV reverse transcriptase.<sup>79–81</sup>

Perhaps the most surprising feature from the A-family polymerase structures is that, in the “open” conformation, the templating base exists in an extrahelical conformation that precludes direct physical interactions with the incoming dNTP. In the case of the *Bacillus stearothermophilus* polymerase, a conserved tyrosine (Tyr-714) stacks within the DNA template and replaces the coding nucleobase. This interaction blocks direct access of the incoming nucleotide with any templating nucleobase.<sup>82,83</sup> Although the templating base is initially positioned in an extrahelical conformation, DNA polymerization still occurs using the crystal of the *B. stearothermophilus* polymerase,<sup>82,83</sup> indicating that this unusual conformation is catalytically active. The transition from “open” to “closed” state is limited to rigid-body motions of the finger subdomain with additional conformational changes in three hinge regions in the fingers.<sup>83</sup> These data suggest that conformational changes can occur within the crystal and function to position the templating base into an intrahelical position that permits phosphoryl transfer to occur. The observation of an extrahelical templating base is not unique to the *B. stearothermophilus* polymerase as structural data from the B-family eukaryotic pol  $\alpha$ <sup>84</sup> and archeal DNA polymerases<sup>85,86</sup> also reveal its existence. In fact, the ternary complex of the RB69 DNA polymerase shows a 90° rotation of the templating base along the DNA backbone, which places the nucleobase in the center of a helix–loop–helix motif constrained by a conserved tyrosine and two conserved glycines.<sup>65</sup>

The presence of an extrahelical templating base is not universal. Crystal structures of the eukaryotic pol  $\beta$ <sup>87,88</sup> and HIV reverse transcriptase,<sup>79–81</sup> both of which have lower fidelity than A- and B-family polymerases, do not show evidence for distortion of the DNA template. In addition, recently published structures of the error-prone DNA polymerase, Dpo4, show that the DNA template exists in a linear conformation as it enters the active site.<sup>89</sup> These observations make it tempting to speculate that positioning of the templating nucleobase in an intrahelical conformation actually has a *negative impact* on fidelity. The provocative implication is that polymerases that rely on forming direct hydrogen bonding contacts between the incoming dNTP and templating base are more likely to display lower fidelity compared to polymerases that avoid direct contacts via distortion of the templating DNA.



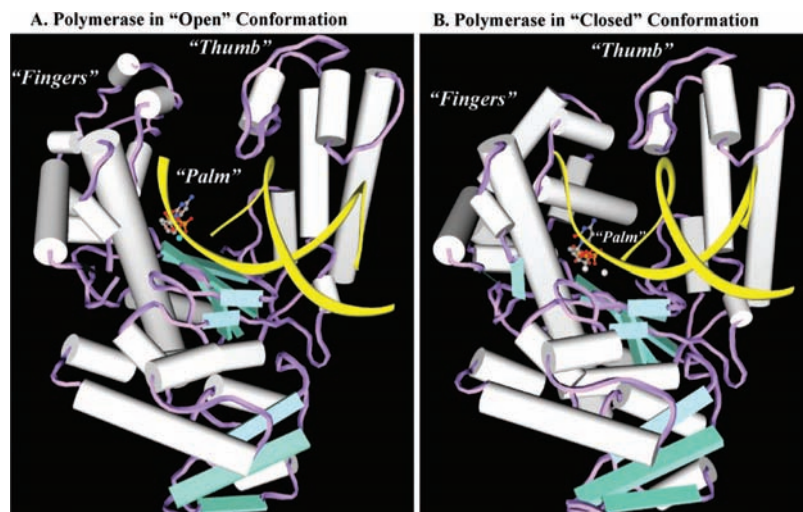


**Figure 7.** Structural models for the large fragment of *Thermus aquaticus* DNA polymerase I (KlenTaq) in an (A) “open” conformation and (B) “closed” conformation. In these projections, the transition of the polymerase from the “open” to “closed” conformation occurs via movement of the fingers subdomain toward the palm subdomain, thereby squeezing the incoming dNTP more tightly into the active site of the polymerase. The ternary complex structures were prepared using the available crystal structures of *Thermus aquaticus* DNA polymerase I and the PDB ID codes 2KTQ (“open”) and 3KTQ (“closed”). MOE (www.chemcomp.com) was used for all structural modeling.

#### 4.6. Kinetic Steps After Phosphoryl Transfer

Following phosphoryl transfer, there is a conformational change step that precedes the release of the first product, PP<sub>i</sub>. After this step, the polymerase presumably translocates to the next templating position, where it can remain bound and continue polymerization on the same nucleic acid substrate or dissociate from the elongated DNA to renew synthesis on another DNA substrate. As described below, the existence of a conformational change following phosphoryl transfer has been demonstrated by examining the reversal of polymerization (vide infra). For now, we focus our attention on the most intriguing and least understood kinetic step in the polymerization cycle—translocation of the polymerase along DNA. Insights into the dynamics of this process have come from structural studies of the *B. steartophilus* DNA polymerase.<sup>82,83</sup> These studies demonstrate successive translocations of the polymerase along DNA duplex after nucleotide incorporation. In addition, it reveals how all four Watson–Crick base pairs exist within the confines of the polymerase’s active site. In general, steric complementarity exists between each Watson–Crick base pair. The conserved geometry of minor groove hydrogen bond acceptors appear to be required for polymerase movement. Despite this structural information, however, the driving force for the translocation event remains enigmatic. Several models have been proposed arguing that polymerase movement is linked with the energy derived from PP<sub>i</sub> release.<sup>90</sup> However, further kinetic and structural studies are needed to fully define the dynamics of polymerase translocation, especially within the context of misreplicating damaged DNA.

#### 4.7. Reversibility of DNA Polymerization

Pyrophosphorolysis is the microscopic reverse of the nucleotide incorporation reaction. This enzymatic activity has been extensively studied since pyrophosphorolysis plays an important role in drug resistance to certain antiviral agents used in the treatment of HIV.<sup>91</sup> By reversing the polymerization reaction, the virally encoded reverse transcriptase (RT) catalyzes the efficient removal of chain-terminating

nucleotide analogues that are designed to inhibit viral DNA synthesis.<sup>92</sup> Removal of the chain-terminator allows viral DNA synthesis to be reinitiated.

The mechanism of pyrophosphorolysis is complex and, in the case of HIV RT, involves the development of several mutations in polymerase’s active site to achieve significant activity required for drug resistance.<sup>93</sup> In this mechanism, RT can position the 3′-OH of the primer into two distinct locations denoted as the priming site (P-site) or the nucleotide-binding site (N-site).<sup>93</sup> During DNA synthesis, RT binds the 3′-OH in the P site while dNTP binding occurs in the N-site. After phosphoryl transfer, the newly extended primer is transferred from the N-site to the P-site so that the catalytic cycle can continue. However, this cycle changes when a chain-terminating nucleotide is incorporated. In the absence of a usable 3′-OH, primer elongation cannot occur such that the binding of the next correct dNTP in the N-site forms a dead-end ternary complex that prohibits viral DNA synthesis. However, the viral polymerase can also partition the chain-terminated primer from the P-site back into the N-site. This favors the binding of PP<sub>i</sub> and allows pyrophosphorolysis to occur. The chain-terminator is then excised to generate dNTP and a viable 3′-OH so that DNA synthesis can resume.

From a mechanistic perspective, an examination of the pyrophosphorolytic activity of the *E. coli* Klenow fragment and bacteriophage T4 DNA polymerase has provided more detailed information regarding the conformational change steps that flank the phosphoryl transfer step. The kinetic parameters of pyrophosphorolysis for either polymerase have been quantified by measuring the rate of appearance of dNTP as a function of different PP<sub>i</sub> concentrations. The  $K_m$  for PP<sub>i</sub> with the Klenow fragment is 230 μM,<sup>94</sup> while that for the T4 polymerase is ~10 mM.<sup>29</sup> Despite the large difference in relatively binding affinity for PP<sub>i</sub>, the maximal rate constant for pyrophosphorolysis,  $k_{\text{pyro}}$ , is similar at 0.3 and 0.5 s<sup>-1</sup> for the Klenow fragment and T4 DNA polymerase, respectively.<sup>29,94</sup> In both cases, the rate constants for pyrophosphorolysis are much slower than the  $k_{\text{pol}}$  values of >50 s<sup>-1</sup> measured for the forward reaction. This indicates that the equilibrium constant for the chemical step is highly

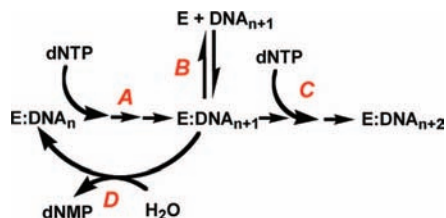


**Figure 8.** Kinetic pathway for the formation and processing of a mismatch. Step A represents formation of the mismatch. Step B represents dissociation of the mismatched DNA from the polymerase. Step C represents the ability of the polymerase to extend beyond the mismatched primer-temple. Step D represents removal of the mismatch via exonucleolytic proofreading.

avored in the direction of polymerization. In addition, a burst in dNTP production caused by pyrophosphorolysis is not detected with the Klenow fragment, indicating the presence of a slow step that follows formation of  $E':DNA_{n+1}:PP_i$  in the direction polymerization.<sup>94</sup>

As previously described, decay of the  $E':DNA_{n+1}:PP_i$  species to generate  $DNA_{n+1}$  and  $PP_i$  can occur via two mutually exclusive pathways. The first involves release of  $PP_i$  from the  $E':DNA_{n+1}:PP_i$  followed by a conformational change that relaxes the resulting  $E':DNA_{n+1}$  species to  $E:DNA_{n+1}$ . The second pathway involves  $PP_i$  release after relaxation of the  $E':DNA_{n+1}:PP_i$  complex to  $E:DNA_{n+1}:PP_i$ . Differentiation between these two mechanisms was achieved by comparing the rates of pyrophosphorolysis with pyrophosphate exchange.<sup>95</sup> Pyrophosphate exchange is measured as the rate of  $^{32}P$ -dNTP appearance into a pool of cold dNTP by the addition of  $[^{32}P]PP_i$ . With the *E. coli* Klenow fragment, identical rates in pyrophosphorolysis and pyrophosphate exchange were measured, arguing for the presence of a second conformational change from  $E':DNA_{n+1}:PP_i$  to  $E:DNA_{n+1}:PP_i$  that precedes  $PP_i$  release. If pyrophosphate exchange was faster than pyrophosphorolysis, then  $PP_i$  exchange with the  $E':DNA_{n+1}$  species would have occurred and circumvented the slow reversal of the conformational relaxation step from  $E:DNA_{n+1}:PP_i$  to  $E'DNA_{n+1}:PP_i$ .

## 5. Fidelity of Nucleotide Incorporation

Mutagenesis of an individual's genome often correlates with the development of disease and/or resistance to drugs designed to combat the pathogenic state. The most critical step in mutagenesis arguably occurs during DNA replication and is caused by the misincorporation of a dNTP opposite normal or damaged DNA followed by subsequent elongation beyond the mismatch (Figure 8). In the absence of exogenous DNA damaging agents, mutagenic events rarely occur as indicated by in vitro error rates corresponding to one error per  $10^4$ – $10^6$  bases replicated by high-fidelity DNA polymerases. This degree of fidelity is remarkable since the energy differences between a correct and incorrect base pair are only 1–3 kcal/mol. This low energy difference predicts a high error rate of 1 error per 100 bases replicated.<sup>96</sup> Thus, the remarkable low mutation frequency observed in many organisms must therefore reflect several enzymatic processes that enhance replication fidelity. We describe these enzymatic activities into those that are influenced by the kinetics of nucleotide incorporation versus those that are controlled by nucleotide removal catalyzed by the exonuclease proofreading activity associated with most replicative DNA polymerases.

### 5.1. Forming a Mismatch: Alterations in the Kinetic Steps Associated with Polymerization

A powerful approach toward understanding the mechanism of mutagenesis is to compare and contrast the kinetic behavior of DNA polymerases during nucleotide incorporation opposite a correct (dATP opposite thymine) versus an incorrect (dATP opposite cytidine) pairing partner. The simplest approach is to quantify the rates of nucleotide incorporation in both cases by measuring primer elongation as a function of time. Other analyses involve comparing  $V_{max}/K_m$  values for incorrect versus correct DNA synthesis.  $V_{max}/K_m$  values reflect the apparent second-order rate constant for productive substrate binding and are often associated with the well-known “specificity constant” for an enzymatic reaction. Furthermore, the ratio of  $V_{max}/K_m$  incorrect to  $V_{max}/K_m$  correct provides a factor that indicates the intrinsic fidelity of a DNA polymerase.

The molecular events underlying reductions in misincorporation rates are typically interpreted with respect to perturbations in the formation of correct hydrogen bonds between the incoming dNTP and its mismatched partner. Simply put, the rates for misincorporating a dNTP are slow since the functional groups required for proper Watson–Crick interactions do not line up properly. As outlined in Figure 4, these alterations can perturb ground-state binding (Step 2), reduce the rate of the conformational change (Step 3), and/or reduce the rate of phosphoryl transfer (Step 4). As such, it is often more appropriate to classify discrimination against misincorporation events through perturbations in binding affinity ( $K_d$  effect), reductions in the rate constant for incorporation ( $k_{pol}$  effect), or a combination of the two. For example, misincorporation of dATP opposite C catalyzed by the bacteriophage T4 DNA polymerase is disfavored  $\sim 330\,000$ -fold compared to correct incorporation of dATP opposite T.<sup>97</sup> In this case, the  $K_d$  for dATP incorporation opposite C is  $1\,100\ \mu M$  and is  $>100$ -fold higher than the  $K_d$  of  $10\ \mu M$  measured for dATP incorporation opposite T.<sup>29</sup> In addition, the rate constant of dATP incorporation opposite C is  $\sim 0.03\ s^{-1}$ ,<sup>197</sup> which is  $3\,300$ -fold slower than the  $k_{pol}$  value of  $100\ s^{-1}$  measured for the correct incorporation of dATP opposite T.<sup>29</sup> Despite this reduction, the conformational change preceding the chemistry step remains the rate-limiting step for incorporation. Finally, the catalytic efficiency ( $k_{pol}/K_d$ ) for creating an A:C mismatch is  $27\ M^{-1}\ s^{-1}$ , while that for forming the proper Watson–Crick base pair (A:T) is  $10^7\ M^{-1}\ s^{-1}$ . The difference in catalytic efficiencies corresponds to a predicted error frequency of one mistake every 1 000 000 incorporation events, which is close to the values determined by in vivo measurements using the exonuclease deficient T4 DNA polymerase.<sup>98</sup>

Two major differences in the mechanism for correct versus incorrect DNA synthesis are noted with the *E. coli* Klenow fragment.<sup>99</sup> First, a change in the rate-limiting step occurs during misincorporation in which phosphoryl transfer rather than the conformational change step preceding chemistry limits the overall rate of misincorporation. This is evident by a significant elemental effect of  $>10$  measured for substituting an  $\alpha$ -S-dNTP for  $\alpha$ -O-dNTP during misincorporation compared to a small elemental effect during correct DNA synthesis.<sup>99</sup> In addition, the rate of the second conformational change following misincorporation is slower.<sup>99</sup> This reduction in the second conformational change is proposed to provide a kinetic barrier that prevents elongation

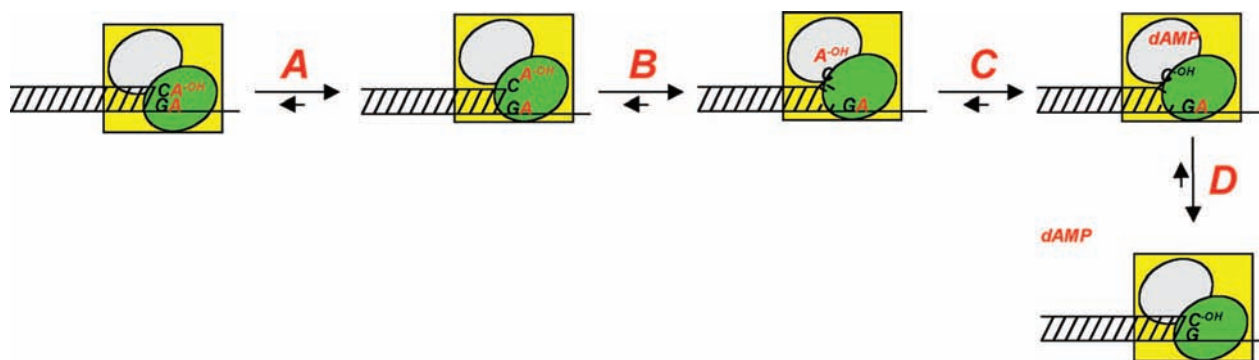


**Figure 9.** Kinetic pathway for the exonuclease proofreading capabilities of the bacteriophage T4 DNA polymerase. Step A represents initial strand separation of mismatched primer template. Step B represents translocation of the primer-terminus from the polymerase active site into the exonuclease active site. Step C represents hydrolysis of the phosphodiester bond to excise the terminal nucleotide. Step D represents repositioning of the 3'-end of the primer from the exonuclease active site back to the polymerase active site.

of the mismatch by allowing the 3'-exonuclease activity of the Klenow fragment to remove the mismatch.<sup>99</sup>

Comparing the kinetic mechanisms of correct and incorrect incorporation for several DNA polymerases has led to a model invoking three distinct stages for maintaining fidelity.<sup>100</sup> The first step occurs during the kinetic step encompassing dNTP binding and phosphodiester bond formation. During this stage, selectivity of  $10^4$ – $10^6$  is achieved. With polymerases such as the *E. coli* Klenow fragment, the contribution of a second conformational change step adds another  $\sim 60$ -fold selectivity by providing additional time to excise mismatches before DNA dissociation (Stage 2). As discussed below, the final stage of selectivity occurs via a  $\sim 10$ – $100$ -fold reduction in the rate for extending a mismatch compared to extending a correctly paired primer-terminus. The combination of all three stages predicts an overall selectivity of 1 error per every  $10^{10}$  opportunities during correct DNA synthesis.

## 6. Processing a Mismatch

If the polymerase does misincorporate, additional macroscopic steps illustrated in Figure 8 contribute to further reducing the error frequency. One obvious kinetic step is polymerase dissociation from DNA after misinsertion (Figure 8, Step B) caused by the altered geometry of the formed mispair.<sup>101</sup> The net effect is that the extension beyond the mismatch is prevented so that the mismatch can be removed by various cellular nucleases. However, most replicative polymerases possess accessory proteins that increase the processivity of the polymerase and, thus, reduce the frequency of dissociation.<sup>48–50</sup> The increased processivity predicts that the polymerase would be forced to extend beyond the mismatch rather than dissociate (Figure 8, Step C). However, this mechanism appears inaccurate since the efficiency for elongating a formed mismatch is reduced compared to extending beyond a correct base pair.<sup>102,103</sup> The reduced rate of extension for a mispair provides an opportunity for the primer-terminus to be processed by exonuclease activity.

### 6.1. Role of Exonuclease Proofreading in Maintaining Genomic Fidelity

The last line of defense to prevent misincorporation is through the proofreading capacity of the DNA polymerase catalyzed by its associated exonuclease activity (Figure 8, Step D). The proofreading process is more complicated as

it encompasses translocation of the primer-terminus from the polymerase active site into the exonuclease active site, strand separation of several nucleotides, positioning of the 3'-end of the primer in the exonuclease active site, and hydrolysis of the phosphodiester bond to excise the terminal nucleotide (Figure 9). In addition to erasing the mismatch, proofreading also returns the polymerase to a correct primer-terminus, which allows for the renewal of “correct” DNA synthesis without polymerase dissociation and rebinding.

### 6.2. Chemistry of Exonuclease Proofreading

Exonuclease proofreading activity has been extensively studied using the bacteriophage T4 enzyme as the model system.<sup>104–109</sup> The primary advantage of this system has been the ability to combine classical genetic selection with site-directed mutagenesis to rapidly screen a variety of mutant DNA polymerases possessing defects in 3'→5' exonuclease activity.<sup>104–109</sup> These studies indicate that exonuclease activity requires the binding of two catalytically important metals through conserved carboxylates.<sup>105–108</sup> In vivo analyses reveal that the D324A, D219A and D112A/E114A mutant T4 DNA polymerases are defective in 3'→5' exonuclease activity and have a 1 000-fold increase in the development of spontaneous mutations compared to wild-type polymerase.<sup>108</sup> In vitro analyses confirm that D324 binds one of the required metal ions and is the single-most important amino acid for the hydrolysis reaction.<sup>108</sup> The exonuclease activity of the D324A mutant is  $10^5$ -fold lower than wild-type polymerase, while reductions of  $10^3$ - to  $10^4$ -fold have been reported for the D219A- and D112A/E114A-DNA polymerases, respectively. pH studies of exonuclease activity suggest that a water molecule coordinated by one metal ion forms a metal-hydroxide ion that is oriented to attack the phosphodiester bond.<sup>109</sup>

### 6.3. Kinetic Mechanism of Nucleotide Excision

Mismatched DNA is the preferred substrate for exonuclease activity as rates for excising mismatched base pairs are 100-fold higher than for correctly matched base pairs.<sup>109</sup> The overall mechanism for nucleotide excision involves a competition between the enzyme's polymerase and exonuclease active sites for the 3'-end of the primer strand.<sup>109</sup> As outlined above, polymerization is stalled after formation of the mismatch due to misorientation of the 3'-hydroxyl group of the primer-terminus that subsequently hinders the incorporation of the next correct nucleotide. Polymerase stalling

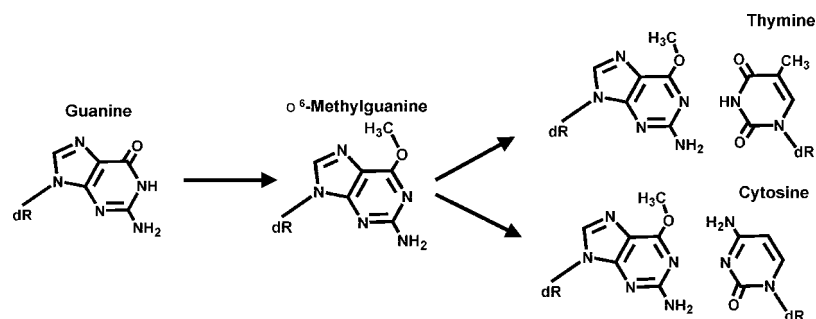


**Figure 10.** Formation of O<sup>6</sup>-methylguanine and consequences of misreplicating the miscoding DNA lesion.

increases the probability of excision due to shuttling of the mispaired primer away from the polymerization domain. In addition, a mismatched base pair destabilizes duplex DNA and enhances the binding of the partially melted 3'-single-stranded primer into the exonuclease site.

The details of the kinetic mechanism for the proofreading pathway of bacteriophage T4 DNA polymerase have been elucidated through presteady-state kinetic studies<sup>29,109</sup> coupled with mutational analyses.<sup>105–108</sup> As illustrated in Figure 9, polymerase stalling at the mismatch allows the enzyme to first partially melt the primer-terminus, which facilitates transfer of the primer from the polymerase active site into a pre-exonuclease complex (Step A). This appears to be the rate-limiting step for the proofreading pathway since stopped-flow fluorescence analysis with 2-AP containing DNA shows that this step occurs with a rate constant,  $k_1$ , of  $\sim 4 \text{ s}^{-1}$ , which is essentially identical to that of  $5 \text{ s}^{-1}$  measured using rapid-quench techniques.<sup>29</sup> Further strand separation (Step B) forces the primer-terminus to bind in the exonuclease active site and occurs with a faster rate constant,  $k_2$ , of  $\sim 20 \text{ s}^{-1}$ . Finally, hydrolysis of the phosphodiester bond (Step C) occurs with a fast rate constant of  $\sim 100 \text{ s}^{-1}$ . Repositioning of the primer in the polymerase active site is rapid (Step D). It is important to emphasize that both Steps A and B are significantly slower than either the hydrolysis rate constant of  $100 \text{ s}^{-1}$  measured for Step C or the rate constant of  $\sim 400 \text{ s}^{-1}$  measured for extending a correct base pair (28). These differences provide kinetic evidence for the formation of proofreading intermediates generating kinetic barriers that prevent indiscriminate excision of correctly base-paired DNA.

In addition, this kinetic barrier allows for idle turnover, the process of repetitive addition, excision, and addition of a dNTP. This activity not only inhibits mispair elongation but allows the DNA polymerase to remain “stalled” on DNA. This activity may act to coordinate replication with other biological pathways including DNA repair, DNA recombination, and/or the bypass of certain DNA lesions.

## 7. Polymerase Activity is Altered by DNA Damage

DNA damaging agents such as temozolomide, chlorambucil, and cisplatin are widely used in the treatment of various cancers including brain tumors, ovarian and prostate cancers, malignant melanomas, and hematological disorders.<sup>110</sup> By damaging DNA, these agents block replication and transcription as well as activate DNA repair pathways to induce apoptosis.<sup>111</sup> Unfortunately, the DNA lesions caused by these agents can be misreplicated to generate resistance as well as to create potential genetic errors. Indeed, translesion DNA synthesis, the ability of a DNA polymerase to replicate damaged DNA and extend it, represents a major

complication in the widespread use of DNA damaging agents. In the following sections, we examine the effects of various DNA lesions on the mechanism and fidelity of various DNA polymerases.

### 7.1. Miscoding DNA Lesions

O<sup>6</sup>-methylguanine (O<sup>6</sup>-MeG) is a prototypical miscoding DNA lesion that is caused by alkylating agents including methyl methanesulfonate<sup>112</sup> and chemotherapeutic agents such as temozolomide<sup>113</sup> and cyclophosphamide.<sup>114</sup> As illustrated in Figure 10, this lesion is potentially miscoding since alkylation at the O6-position of guanine changes the hydrogen bonding potential of the nucleobase through modification to the keto oxygen. This modification changes the Watson–Crick hydrogen bonding pattern of guanine from **a\*d\*d** to **(-)\*a\*d** such that it now resembles adenine rather than guanine.

Nucleotide incorporation opposite O<sup>6</sup>-MeG has been quantified using several different DNA polymerases, including the *E. coli* Klenow fragment<sup>115</sup> and bacteriophage T4 DNA polymerase.<sup>116,117</sup> Using the exonuclease-deficient *E. coli* Klenow fragment, Spratt and Levy reported that the catalytic efficiency for dTTP incorporation is 3-fold higher than that for dCTP.<sup>115</sup> The preferential incorporation of dTTP does not arise through an effect on nucleotide binding since the  $K_m$  values for dTTP and dCTP are identical at  $\sim 100 \mu\text{M}$ . Instead, the higher catalytic efficiency reflects the faster  $k_{\text{cat}}$  value measured for dTTP incorporation. The T4 DNA polymerase likewise shows a preference for incorporating dTTP rather than dCTP opposite O<sup>6</sup>-MeG.<sup>116,117</sup> Presteady-state analyses reveal that the binding affinity for dCTP is significantly higher compared to that for dTTP (A. Berdis, unpublished results). However, the higher catalytic efficiency for dTTP incorporation arises from a 10-fold faster rate constant for incorporations compared to that for dCTP incorporation (A. Berdis, unpublished results). In addition, the polymerase extends beyond the T:O<sup>6</sup>-MeG base pair more efficiently compared to the C:O<sup>6</sup>-MeG mispair,<sup>117</sup> even in the presence of exonuclease proofreading<sup>117</sup> (A. Berdis, unpublished results). Collectively, the *in vitro* demonstration for the preferential incorporation and extension of dTTP opposite O<sup>6</sup>-MeG is consistent with *in vivo* observations of the pro-mutagenic potential of this lesion.

### 7.2. Non-Instructional DNA Lesions

Perhaps the most prevalent and pro-mutagenic class of DNA lesion is an abasic site (Figure 11). This noninstructional DNA lesion is formed by the hydrolysis of the bond between the C1' of ribose and the N9 of a purine or the N1 of a pyrimidine. Although abasic sites arise spontaneously

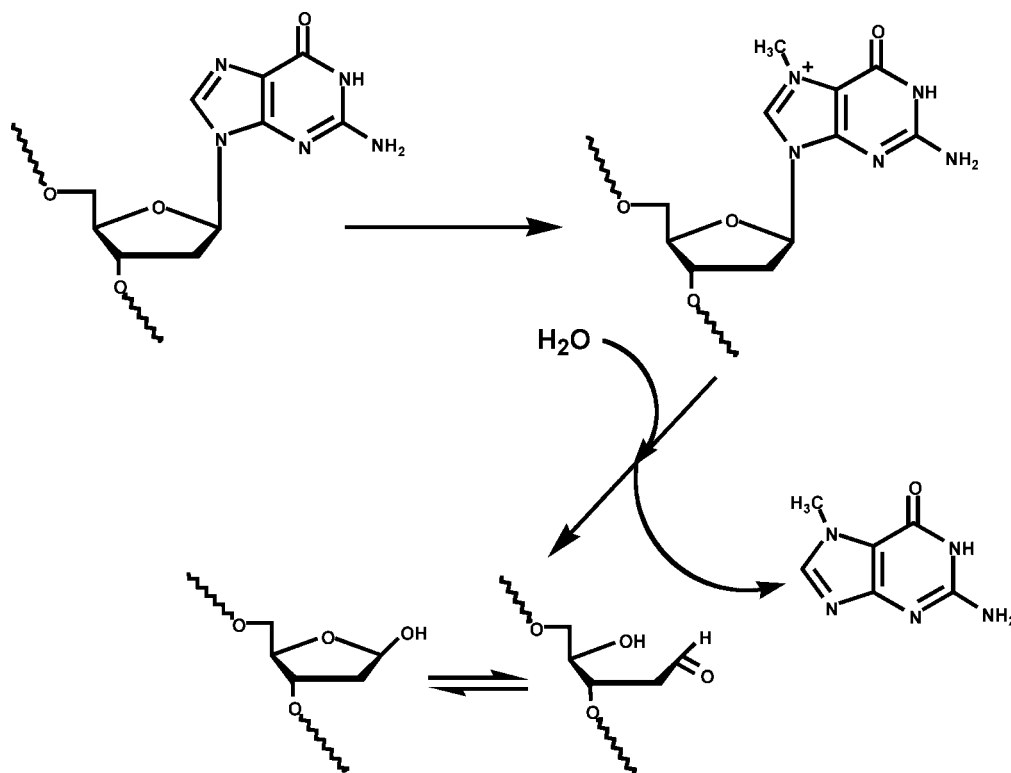


**Figure 11.** Nonenzymatic formation of an abasic site, a noninstructional DNA lesion.

under normal physiological conditions,<sup>118</sup> their formation is enhanced by exposure to ionizing radiation and chemotherapeutic agents<sup>119</sup> as well as through the action of DNA glycosylases that excise damaged nucleobases.<sup>120</sup> While most abasic sites are repaired by the base excision repair pathway,<sup>121</sup> a small fraction persist and can be replicated to yield a high probability of mutagenesis. The lack of coding information at an abasic site predicts that all four dNTPs should be incorporated with equal efficiencies and forecasts a 75% chance for a misincorporation event that could cause a genetic mutation. Despite the lack of coding information present at an abasic site, however, high fidelity DNA polymerases such as eukaryotic pol  $\delta$ ,<sup>122</sup> the *E. coli* Klenow fragment,<sup>123</sup> and the bacteriophage T4 DNA polymerase<sup>124</sup> preferentially insert dATP opposite the lesion. This kinetic phenomenon is commonly referred to as the “A-rule” of translesion DNA synthesis.<sup>125</sup>

The mechanism for misreplicating an abasic site has been extensively studied using the bacteriophage T4 DNA polymerase<sup>124</sup> and Klenow fragment<sup>123</sup> as models. With the T4 polymerase, the catalytic efficiency for incorporating dATP opposite the lesion is  $\sim 100$ -fold higher than that for the other three natural dNTPs.<sup>124</sup> The higher efficiency results from a significant increase in binding affinity coupled with a faster  $k_{\text{pol}}$  value.<sup>124</sup> It is surprising that the binding affinity for dATP opposite the lesion is only 3-fold worse than that for incorporation opposite the correct pairing partner thymine. Instead, the most sensitive parameter is the  $k_{\text{pol}}$  value, which is decreased from  $100 \text{ s}^{-1}$  during correct incorporation opposite thymine to  $0.15 \text{ s}^{-1}$  for insertion opposite an abasic site.<sup>124</sup> Thus, discrimination is caused by a 1 000-fold reduction in the  $k_{\text{pol}}$  value rather than perturbations in binding affinity. This is consistent with the induced-fit model for polymerase fidelity<sup>29</sup> because the rate-limiting step for nucleotide incorporation is the conformational change step preceding phosphoryl transfer as validated by thio-elemental

effects studies,<sup>124</sup> pulse-chase experiments,<sup>126</sup> and fluorescence measurements of nucleotide incorporation.<sup>127</sup> Furthermore, extension beyond an abasic site is reduced  $\sim 1\ 000$ -fold compared to extension beyond a correct base pair.<sup>124</sup> Surprisingly, the kinetics of elongation appear to be limited by the phosphoryl transfer step based upon the observation of a significant ( $>10$ -fold) thio-elemental effect.<sup>128</sup>

The *E. coli* Klenow fragment is similar to the bacteriophage T4 DNA polymerase in that it also incorporates dATP  $\sim 10$ -fold more efficiently opposite an abasic site compared with any other natural nucleotide.<sup>123</sup> This suggests that the mechanism of translesion DNA replication is identical between these polymerases. However, subtle differences in the measured kinetic parameters argue otherwise. Specifically, the Klenow fragment binds dATP 4-fold weaker compared to the T4 polymerase. In addition, the maximal rate constant for incorporating dATP is 5-fold faster with Klenow fragment than with the bacteriophage polymerase. Furthermore, significant differences in the kinetic parameters for various non-natural nucleotides have been reported,<sup>123</sup> indicating that the mechanism of nucleotide incorporation opposite an abasic site differs between DNA polymerases. The differences observed during the misreplication of damaged DNA emphasize the subtleties employed during nucleotide incorporation to maintain genomic fidelity.<sup>123</sup>

### 7.3. Replication of Bulky DNA Lesions

Numerous types of bulky lesions have been identified both in vitro and in vivo.<sup>130</sup> However, thymine dimers and cisplatin-induced DNA cross-links (Figure 12) are two of the most extensively studied lesions due to their importance in cancer. Although the primary causative agent of skin cancer is solar UV light, DNA lesions such as thymine dimers and other dipyrimidine photoproducts are the direct cause for mutagenesis associated with cancer initiation.<sup>129</sup>

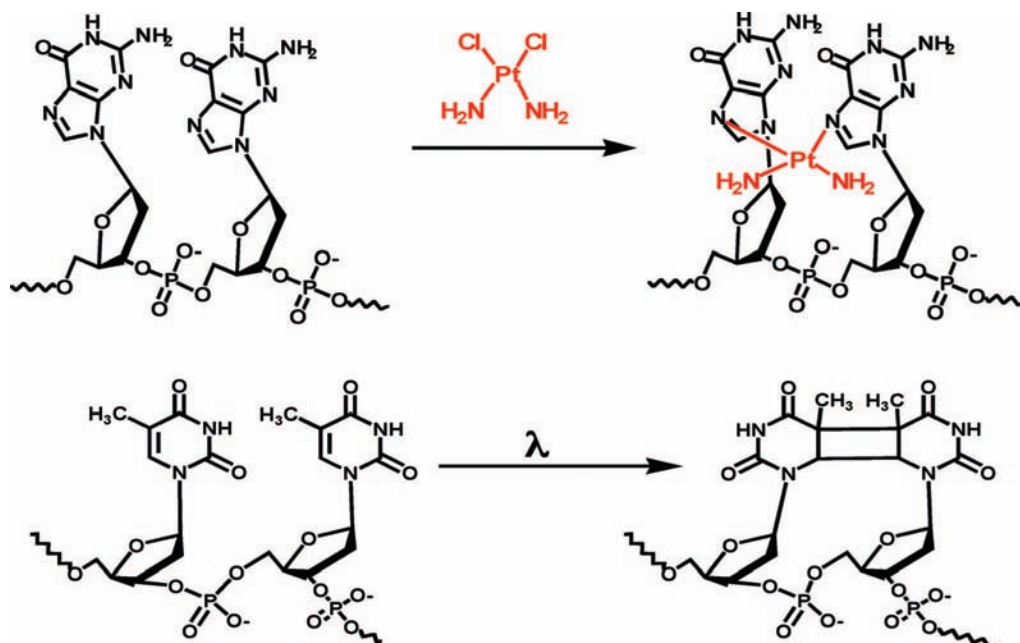


**Figure 12.** Structures of bulky DNA lesions such as (A) cisplatinated guanines and (B) a thymine dimer. See text for discussion on the formation and effects of these lesions of the efficiency and fidelity of DNA replication.

At the other end of the spectrum is *cis*-diaminedichloro-platinum(II) (cisplatin), a widely used anticancer drug that reacts with adjacent guanine bases in DNA to predominantly form intrastrand cross-links. The sheer bulk of this DNA lesion provides a significant roadblock that impedes the synthetic capabilities of various DNA polymerases and causes cytostatic and cytotoxic effects. The following sections describe the influence of these bulky DNA adducts on the mechanism and fidelity of DNA polymerases.

#### 7.4. Thymine Dimers

UV radiation causes a variety of covalently modified DNA lesions. However, the most prevalent form of damage is the *cis,syn*-thymine dimer. Although thymine dimers are repaired by several distinct DNA repair pathways,<sup>130</sup> they are also inappropriately replicated by various DNA polymerases.<sup>131–133</sup> As illustrated in Figure 12, the hydrogen bonding groups required for base-pair recognition are not altered at a thymine dimer. Instead, this lesion induces various deformations in the helical structure of DNA<sup>134</sup> that are proposed to create a cavity that functionally resembles the noninstructional abasic site. Indeed, recent studies reveal that high-fidelity DNA polymerases replicate a thymine dimer more similarly to a noninstructional lesion rather than as a miscoding lesion.<sup>135</sup> This model for misreplication was first proposed based upon structural evidence of the bacteriophage T7 DNA polymerase when bound to a thymine dimer.<sup>135</sup> In this structure, the polymerase places the lesion outside the helical structure of DNA to create a cavity that mimics an abasic site.<sup>135</sup> This mechanism was subsequently confirmed by kinetic studies demonstrating that the T7 DNA polymerase preferentially incorporates a non-natural nucleotide, pyrene triphosphate, rather than dATP opposite the thymine dimer DNA lesion and is similar to the kinetic preference displayed at an abasic site.<sup>136</sup>

The mechanism for replicating a thymine dimer has also been investigated using a series of non-natural nucleotides with the bacteriophage T4 DNA polymerase.<sup>137</sup> Results from these studies demonstrate that this high-fidelity DNA poly-

merase replicates a thymine dimer via a mechanism that is similar, but not identical, to that reported for the misreplication of an abasic site.<sup>134,137</sup> The catalytic efficiency for nucleotide incorporation opposite both lesions is linked with the overall  $\pi$ -electron surface area of the incoming nucleotide. However, the rate constant for the conformational change step at a thymine dimer is considerably slower than those measured at an abasic site. This difference likely reflects the influence of steric hindrance imposed by the bulky lesion. Data from these kinetic studies were interpreted with a model in which the 3'-T of the lesion exists predominantly in an extrahelical position that creates an intermediate resembling an abasic site.<sup>137</sup> However, the covalent bond between the 5'-T and 3'-T hinders the overall mobility of the lesion such that the rate constant for the conformational change step preceding phosphoryl transfer is significantly slower compared to that for a genuine abasic site.

Despite differences in the mechanism of nucleotide incorporation between an abasic site or thymine dimer, the T4 DNA polymerase processes mismatches present at either lesion similarly with respect to extension and exonuclease proofreading. Extension beyond both DNA lesions is inefficient and reduced 1,000-fold compared to extension beyond a correct base pair.<sup>123,137</sup> In addition, the kinetics for excising dAMP from either DNA lesion are identical and significantly faster than dAMP excision from an unmodified thymine.<sup>123,137</sup> This enhancement likely reflects the enzyme's ability to partition the misaligned primer from the polymerase active site into its exonuclease domain and contributes toward the lack of extension beyond either mispair.

#### 7.5. Replication of Cisplatin-Modified DNA

The effects of a site-specific cisplatin adduct on DNA polymerization have been investigated using two replicative DNA polymerases, HIV RT, and the bacteriophage T7 DNA polymerase.<sup>138</sup> HIV RT binds cisplatin-containing DNA with a similar affinity to unmodified DNA, whereas the T7 DNA polymerase binds the cisplatin-DNA cross-link with significantly worse affinity. However, both polymerases show

strong pausing at the cross-linked guanine as well as one nucleotide preceding the DNA lesion.<sup>138</sup> Single nucleotide incorporation at each pause site revealed that polymerization occurs with biphasic kinetics, which is consistent with the previously described two-step reaction mechanism outlined for correct DNA synthesis. However, the burst amplitudes in nucleotide incorporation opposite the damaged DNA are significantly smaller than expected. This indicates that the polymerases bind the lesion nonproductively compared to unmodified DNA. In addition, both polymerases extend beyond the lesion  $\sim 10^4$ -fold more slowly compared to unmodified DNA. In this case, the cisplatin lesion has large downstream effects on the kinetics of nucleotide incorporation with the T7 DNA polymerase because ground-state binding for the next correct nucleotide is weakened by the adduct. HIV RT, however, appears to be more tolerant since the binding affinity for nucleotide substrates remain unaffected at downstream positions. This difference may reflect the ability of HIV RT to utilize diverse nucleic acid substrates that include RNA/RNA, DNA/RNA, and DNA/DNA.<sup>139</sup>

Collectively, the inability of high-fidelity polymerases to efficiently incorporate dNTPs opposite bulky lesions such as thymine dimers and cisplatin-induced adducts reflects an important step in preventing the generation of mutations during chromosomal DNA synthesis. As described below, these DNA-replication blocks can be rescued by the activity of various damage-responsive DNA polymerases.

## 8. Damage-Responsive DNA Polymerases

There exist a wide variety of specialized DNA polymerases, known as translesion or damage-responsive DNA polymerases, that can overcome the replication blocks caused by DNA damaging agents.<sup>140–142</sup> These polymerases are enigmatic as they display extremely low fidelity while replicating undamaged DNA yet show surprisingly high fidelity when replicating damaged DNA. Indeed, these polymerases display paradoxical effects in vivo as their uncontrolled participation in normal DNA synthesis presents a threat to genome stability.<sup>143</sup> However, their absence in response to DNA damage is linked with mutagenesis and disease development.<sup>144</sup> The following sections explore this interesting paradox by examining the activity of various translesion DNA polymerases toward replicating abasic sites, thymine dimers, and cisplatin-modified DNA.

### 8.1. Replication of Abasic Sites

While high-fidelity DNA polymerases preferentially incorporate dATP opposite an abasic site, several error-prone polymerases prefer to incorporate other natural nucleotides. For example, pol  $\iota$  preferentially incorporates dGTP opposite this noninstructive DNA lesion by actively discriminating against dATP incorporation.<sup>140</sup> Another polymerase that defies the “A-rule” is the yeast Rev1 DNA polymerase that preferentially incorporates dCTP opposite the noninstructive lesion.<sup>141</sup> Rev1 is unique because it is highly specialized for the insertion of dCTP opposite a variety of DNA lesions including abasic sites and modified guanines.<sup>145</sup> The ternary crystal structure of yeast Rev1 bound to DNA and dCTP reveals that the polymerase does not use the coding information provided by the DNA substrate.<sup>146</sup> Instead, the polymerase uses hydrogen bonding interactions provided by active site amino acids to guide the preferential incorporation of dCTP.<sup>147</sup> In this mechanism, the templating nucleobase

is “flipped” out of the DNA helix such that the incoming dCTP pairs with an active site arginine rather than the templating base. This mechanism ensures that dCTP is preferentially incorporated and provides an efficient way to catalyze error-free DNA synthesis on modified guanine residues.

### 8.2. Damage-Responsive DNA Polymerase Replicate Bulky DNA Lesions with High Fidelity

Damage-responsive polymerases such as pol  $\eta$  catalyze efficient and error-free replication through thymine dimers and other types of bulky lesions. The participation of pol  $\eta$  in translesion DNA synthesis is best understood by its role in the UV-sensitivity syndrome, xeroderma pigmentosum-variant (XP-V).<sup>147</sup> Mutation of the *POLH* gene encoding pol  $\eta$  is linked with the inability to accurately bypass UV-induced cyclobutane pyrimidine dimers.<sup>147</sup> Furthermore, complete inactivation of pol  $\eta$  in humans results in cancer-prone syndrome, a variant form of xeroderma pigmentosum.<sup>148</sup>

Mechanistic studies reveal that pol  $\eta$  is insensitive to distortions in the geometry of the lesion and directly incorporates nucleotides opposite the thymine dimer using the intrinsic base-pairing capabilities of the DNA lesion.<sup>149</sup> Crystallographic studies of another error-prone polymerase, Dpo4, complexed with a *cis,syn*-thymine dimer reveals that the 3′-T of the dimer forms a Watson–Crick base pair with the correct pairing partner, dATP.<sup>150</sup> While the 5′-T is also replicated faithfully, there are significant differences in the mechanism of nucleotide incorporation. Specifically, the 5′-T forms a Hoogsteen base pair with dATP in *syn*- rather than *anti*- conformation.<sup>150</sup>

Pol  $\eta$  can bypass other DNA damage adducts including those induced by cisplatin.<sup>151</sup> Recent structural data reveals that pol  $\eta$  binds the cisplatin lesion in an open conformation.<sup>152</sup> Nucleotide incorporation requires that the lesion rotate into an active conformation in a process that is driven by the formation of Watson–Crick hydrogen bonds between the 3′-G of the lesion and dCTP. While the 3′-G is accurately replicated, bypass of the 5′-G is less efficient and more promiscuous as dATP is incorporated with an efficiency similar to that of dCTP.<sup>152</sup> The facile incorporation of dATP may be caused by the formation of a “transient-abasic site” intermediate as proposed for the cross-linked thymine dimer since the bulky lesion may be unable to fit within the active site of the “error-prone” polymerase.

It is argued that drug resistance to cisplatin arises from the ability of pol  $\eta$  to perform translesion synthesis beyond the cross-linked DNA adducts.<sup>153,154</sup> XP-V cell lines that are defective in pol  $\eta$  are significantly more sensitive to cisplatin treatment compared to isogenic cell lines complemented with functional pol  $\eta$ .<sup>153</sup> Similar results were obtained with the DNA damaging agents, carboplatin and oxaliplatin,<sup>153</sup> and collectively suggest that pol  $\eta$  activity is absolutely required to provide tolerance to platinum-based drugs. In addition, a recent report by Albertella et al.<sup>154</sup> reveals that a lack of pol  $\eta$  expression causes an increase in cisplatin-induced S-phase arrest. This suggests that the inability to perform translesion DNA synthesis causes cell-cycle arrest and argues that pol  $\eta$  activity is an important determinant of cellular responses to cisplatin.

A provocative implication of these studies is that modulating the activity of this error-prone polymerase could provide a beneficial response to platinum-based chemotherapeutic agents. Support for this argument comes from in situ studies

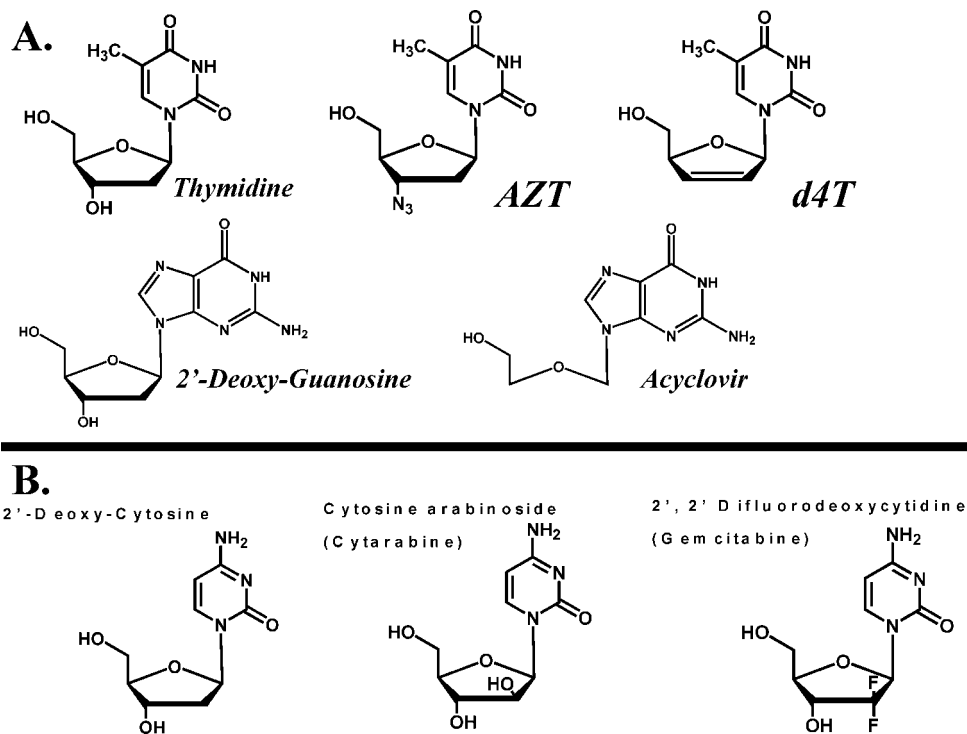


**Figure 13.** Structures of various nucleoside analogues that function as (A) antiviral and (B) anticancer agents. See text for further details regarding their mechanism of action.

demonstrating that pol  $\eta$ -deficient cells are  $\sim 10$ -fold more sensitive to the combined treatment of cisplatin and gemcitabine compared to normal human fibroblast cells.<sup>154</sup> Biochemical analyses suggest that the increased sensitivity to this drug combination reflects the inability of the pol  $\eta$ -deficient cells to restart stalled DNA synthesis presumably caused by the incorporation of gemcitabine opposite cisplatin-induced DNA adducts.<sup>153</sup> Thus, inhibiting pol  $\eta$  may provide a new strategy to improve the effectiveness and potency of existing chemotherapeutic agents that damage DNA.

## 9. Therapeutic Interventions

This kinetic framework highlights the importance of various enzymatic steps that can be exploited to inhibit DNA polymerases to influence cellular proliferation. The current paradigm for therapeutic intervention is the use of chain-terminating nucleotides that are efficiently incorporated into DNA but cannot be extended. As previously outlined,<sup>155</sup> the development of an effective chain-terminating nucleotide depends upon several interrelated features that include (i) high catalytic efficiency for incorporation, (ii) no potential for subsequent elongation, (iii) poor excision after incorporation, (iv) selective utilization by the polymerase(s) responsible for the pathogenic state, and (v) efficient metabolism of the parental nucleoside to the corresponding nucleoside triphosphate. Figure 13 compares the structures of several therapeutically relevant nucleoside analogues that are used as antiviral or anticancer agents. A common feature that distinguishes most antiviral nucleoside analogues (Figure 12A) from their natural counterparts is the absence of the 3'-OH group that is required for primer elongation after incorporation. For example, AZT-TP is an effective chain-terminator due to the simple replacement of the hydroxyl group with an azide ( $-\text{N}_3$ ). Since the coding potential of the antiviral agent is not altered, the overall catalytic

efficiency ( $k_{\text{pol}}/K_{\text{d}}$  value) for a modified nucleotide is comparable to its natural counterpart.<sup>156–158</sup> Nucleoside analogues such as fludarabine, gemcitabine, and cytarabine (Figure 12B) represent an important class of chemotherapeutic agents used mainly in the treatment of hematological disorders.<sup>159</sup> Their mechanism of action is similar to previously discussed antiviral agents such as AZT because the ribose moiety that is essential for primer elongation is modified compared to the natural nucleoside. A major difference, however, is that the deoxyribose sugar is replaced with arabinose or some other modified sugar. This simple replacement make these analogues effective anticancer agents through multiple mechanisms that include direct inhibition of DNA and RNA synthesis as well as altering intracellular nucleotide pools.<sup>160</sup>

## 10. Conclusions

DNA replication is a key biological process that is essential for the survival of any organism and for the proliferation of a species. The ability of a DNA polymerase to accurately copy an organism's genome is of paramount importance in the process. Numerous biophysical, kinetic, and structural studies have provided key insight into the mechanism and dynamics of DNA polymerization. Mechanistic studies reveal that the efficiency and fidelity of replicative DNA polymerases is achieved through a series of conformational changes within the polymerase and DNA that enhance incorporation of the correct nucleotide and prevent misinsertion of an incorrect nucleotide. Surprisingly, there is significant structural evidence indicating that this process is not dependent upon initial hydrogen-bonding contacts made between the incoming nucleotide and the templating nucleobase. As expected, DNA damaging agents, especially those used in chemotherapy, alter the mechanism and dynamics of DNA replication. In some cases, lesions are misreplicated via the inappropriate action of high-fidelity DNA poly-



merases involved in chromosomal DNA synthesis. Surprisingly, error prone polymerases are intimately involved in replicating damaged DNA and ironically appear to be essential for maintaining genomic fidelity in the presence of DNA damage. While we understand the function of DNA polymerases at the cellular and molecular levels, we are just beginning to elucidate the intimate details of how they interact with each other to coordinate DNA synthesis.

## 11. References

- (1) Sawyer, R. D. *The Art of War*; Westview Press: Boulder, CO, 1994; p 3.
- (2) Stillman, B. *FEBS Lett.* **2005**, *579*, 877.
- (3) Johnson, A.; O'Donnell, M. C. *Annu. Rev. Biochem.* **2005**, *74*, 283.
- (4) Bartek, J. L.; Lukas, J. *Curr. Opin. Cell. Biol.* **2007**, *19*, 238.
- (5) Skarstad, K.; Wold, S. *Mol. Microbiol.* **1995**, *17*, 825.
- (6) Mitra, R.; Pettitt, B. M.; Rame, G. L.; Blake, R. D. *Nucleic Acids Res.* **1993**, *21*, 6028.
- (7) Goodman, M. F.; Fyngenson, K. D. *Genetics* **1998**, *148*, 1475.
- (8) Kunkel, T. A.; Bebenek, K. *Annu. Rev. Biochem.* **2000**, *69*, 497.
- (9) The only DNA polymerase identified to date that catalyzes template-independent DNA synthesis under in vivo conditions is terminal deoxynucleotidyl transferase. This polymerase displays the unusual ability to incorporate nucleotides in a random fashion using only single-stranded DNA as the nucleic acid substrate.
- (10) Knowles, J. R. *Annu. Rev. Biochem.* **1980**, *49*, 877.
- (11) Steitz, T. A. *J. Biol. Chem.* **1999**, *274*, 17395.
- (12) Garcia-Diaz, M.; Bebenek, K.; Krahn, J. M.; Pedersen, L. C.; Kunkel, T. A. *DNA Repair (Amst)* **2007**, *6*, 1333.
- (13) Cisneros, G. A.; Perera, L.; García-Díaz, M.; Bebenek, K.; Kunkel, T. A.; Pedersen, L. G. *DNA Repair (Amst)* **2008**, *7*, 1824.
- (14) Sucato, C. A.; Upton, T. G.; Kashemirov, B. A.; Batra, V. K.; Martínek, V.; Xiang, Y.; Beard, W. A.; Pedersen, L. C.; Wilson, S. H.; McKenna, C. E.; Florián, J.; Warshel, A.; Goodman, M. F. *Biochemistry* **2007**, *46*, 461.
- (15) Fox, M.; Brennand, J. *Carcinogenesis* **1980**, *1*, 795.
- (16) Boiteux, S.; Huisman, O.; Laval, J. *EMBO J.* **1984**, *3*, 2569.
- (17) Kelly, J. D.; Shah, D.; Chen, F. X.; Wurdeman, R.; Gold, B. *Chem. Res. Toxicol.* **1998**, *11*, 1481.
- (18) Schaaper, R. M.; Glickman, B. W.; Loeb, L. A. *Cancer Res.* **1982**, *42*, 3480.
- (19) Dianov, G. L.; Souza-Pinto, N.; Nyaga, S. G.; Thybo, T.; Stevnsner, T.; Bohr, V. A. *Prog. Nucleic Acid Res. Mol. Biol.* **2001**, *68*, 285.
- (20) Krokan, H. E.; Nilsen, H.; Skorpen, F.; Otterlei, M.; Slupphaug, G. *FEBS Lett.* **2000**, *476*, 73.
- (21) Boiteux, S.; Guillet, M. *DNA Repair (Amst)* **2004**, *3*, 1.
- (22) Wilson, D. M.; Bohr, V. A. *DNA Repair (Amst.)* **2007**, *6*, 544.
- (23) McClure, W. R.; Jovin, T. M. *J. Biol. Chem.* **1975**, *250*, 4073.
- (24) Bryant, F. R.; Johnson, K. A.; Benkovic, S. J. *Biochemistry* **1983**, *22*, 3537.
- (25) Chang, L. M. *J. Mol. Biol.* **1975**, *93*, 219.
- (26) Kuchta, R. D.; Mizrahi, V.; Benkovic, P. A.; Johnson, K. A.; Benkovic, S. J. *Biochemistry* **1987**, *26*, 8410.
- (27) Kuchta, R. D.; Benkovic, P.; Benkovic, S. J. *Biochemistry* **1988**, *27*, 6716.
- (28) Wong, I.; Patel, S. S.; Johnson, K. A. *Biochemistry* **1991**, *30*, 526.
- (29) Capson, T. L.; Peliska, J. A.; Kaboord, B. F.; Frey, M. W.; Lively, C.; Dahlberg, M.; Benkovic, S. J. *Biochemistry* **1992**, *31*, 10984.
- (30) Patel, P. H.; Loeb, L. A. *Proc. Natl. Acad. Sci. U.S.A.* **2000**, *97*, 5095.
- (31) Suzuki, M.; Yoshida, S.; Adman, E. T.; Blank, A.; Loeb, L. A. *J. Biol. Chem.* **2000**, *275*, 32728.
- (32) Yang, G.; Franklin, M.; Li, J.; Lin, T. C.; Konigsberg, W. *Biochemistry* **2002**, *41*, 10256.
- (33) DeLucia, A. M.; Chaudhuri, S.; Potapova, O.; Grindley, N. D.; Joyce, C. M. *J. Biol. Chem.* **2006**, *281*, 27286.
- (34) Ollis, D. L.; Brick, P.; Hamlin, R.; Xuong, N. G.; Steitz, T. A. *Nature* **1985**, *313*, 762.
- (35) Freemont, P. S.; Friedman, J. M.; Beese, L. S.; Sanderson, M. R.; Steitz, T. A. *Proc. Natl. Acad. Sci. U.S.A.* **1988**, *85*, 8924.
- (36) Yadav, P. N.; Yadav, J. S.; Modak, M. J. *Biochemistry* **1992**, *31*, 2879.
- (37) Beese, L. S.; Derbyshire, V.; Steitz, T. A. *Science* **1993**, *260*, 352.
- (38) Kiefer, J. R.; Mao, C.; Hansen, C. J.; Basehore, S. L.; Hogrefe, H. H.; Braman, J. C.; Beese, L. S. *Structure* **1997**, *5*, 95.
- (39) Hsu, G. W.; Huang, X.; Luneva, N. P.; Geacintov, N. E.; Beese, L. S. *J. Biol. Chem.* **2005**, *280*, 3764.
- (40) Johnson, S. J.; Taylor, J. S.; Beese, L. S. *Proc. Natl. Acad. Sci. U.S.A.* **2003**, *100*, 3895.
- (41) Ho, D. L.; Byrnes, W. M.; Ma, W.; Shi, Y.; Callaway, D. J. E.; Bu, Z. *J. Biol. Chem.* **2004**, *279*, 39146.
- (42) Doublet, S.; Tabor, S.; Long, A. M.; Richardson, C. C.; Ellenberger, T. *Nature* **1998**, *391*, 251.
- (43) Briebe, L. G.; Kokoska, R. J.; Bebenek, K.; Kunkel, T. A.; Ellenberger, T. *Structure* **2005**, *13*, 1653.
- (44) Cook, P. F.; Cleland, W. W. *Enzyme Kinetics and Mechanism*, 1st ed.; Garland Science: New York, 2007; p 25.
- (45) Barman, T. E.; Bellamy, S. R.; Gutfreund, H.; Halford, S. E.; Lionne, C. *Cell. Mol. Life Sci.* **2006**, *63*, 2571.
- (46) Johnson, K. A. *Curr. Opin. Biotechnol.* **1998**, *9*, 87.
- (47) Mace, D. C.; Alberts, B. M. *J. Mol. Biol.* **1984**, *177*, 295.
- (48) Kelman, Z.; Hurwitz, J.; O'Donnell, M. *Structure* **1998**, *6*, 121.
- (49) Sexton, D. J.; Berdis, A. J.; Benkovic, S. J. *Curr. Opin. Chem. Biol.* **1997**, *1*, 316.
- (50) Moldovan, G. L.; Pfander, B.; Jentsch, S. *Cell* **2007**, *129*, 665.
- (51) Eckert, K. A.; Kunkel, T. A. *J. Biol. Chem.* **1993**, *25*, 13462.
- (52) Pelletier, H.; Sawaya, M. R.; Wolffe, W.; Wilson, S. H.; Kraut, J. *Biochemistry* **1996**, *35*, 12742.
- (53) Washington, M. T.; Johnson, R. E.; Prakash, S.; Prakash, L. *J. Biol. Chem.* **1999**, *274*, 36835.
- (54) Hindges, R.; Hübscher, U. *Biol. Chem.* **1997**, *378*, 345.
- (55) Haracska, L.; Acharya, N.; Unk, I.; Johnson, R. E.; Hurwitz, J.; Prakash, L.; Prakash, S. *Mol. Cell. Biol.* **2005**, *25*, 1183.
- (56) Fan, L.; Kim, S.; Farr, C. L.; Schaefer, K. T.; Randolph, K. M.; Tainer, J. A.; Kaguni, L. S. *J. Mol. Biol.* **2006**, *358*, 1229.
- (57) Johnson, K. A. *Methods Enzymol.* **1995**, *249*, 38.
- (58) Francklyn, C. S.; First, E. A.; Perona, J. J.; Hou, Y. M. *Methods* **2008**, *44*, 100.
- (59) A sub-stoichiometric burst in product formation can also be observed. This phenomenon could reflect heterogeneity in DNA substrate and/or polymerase activity, the presence of a readily reversible chemical step, or a kinetic condition in which the rate constant for the burst phase is <10-fold faster than the rate of the second, slower phase.
- (60) Frey, M. W.; Sowers, L. C.; Millar, D. P.; Benkovic, S. J. *Biochemistry* **1995**, *34*, 9185.
- (61) Rachofsky, E. L.; Ross, J. B.; Osman, R. *Comb. Chem. High Throughput Screening* **2001**, *4*, 675.
- (62) Herschlag, D.; Piccirilli, J. A.; Cech, T. R. *Biochemistry* **1991**, *30*, 4844.
- (63) Showalter, A. K.; Tsai, M. D. *Biochemistry* **2002**, *41*, 10571.
- (64) Arndt, J. W.; Gong, W.; Zhong, X.; Showalter, A. K.; Liu, J.; Dunlap, C. A.; Lin, Z.; Paxson, C.; Tsai, M. D.; Chan, M. K. *Biochemistry* **2001**, *40*, 5368.
- (65) It should be noted that the  $K_d$  value reported using this approach is technically a  $K_m$  value. However, if the conformational change preceding phosphoryl transfer is rate-limiting, then the binding of dNTP to the E:DNA complex is in rapid equilibrium. Under these conditions, the  $K_m$  value for the nucleotide approximates a true dissociation constant.
- (66) Wang, J.; Sattar, A. K.; Wang, C. C.; Karam, J. D.; Konigsberg, W. H.; Steitz, T. A. *Cell* **1997**, *89*, 1087.
- (67) Franklin, M. C.; Wang, J.; Steitz, T. A. *Cell* **2001**, *105*, 657.
- (68) Hogg, M.; Wallace, S. S.; Doublet, S. *EMBO J.* **2004**, *23*, 1483.
- (69) Zahn, K. E.; Belrhali, H.; Wallace, S. S.; Doublet, S. *Biochemistry* **2007**, *46*, 10551.
- (70) Beard, W. A.; Wilson, S. H. *Structure* **2003**, *11*, 489.
- (71) Li, Y.; Korolev, S.; Waksman, G. *EMBO J.* **1998**, *17*, 7514.
- (72) Pelletier, H.; Sawaya, M. R.; Kumar, A.; Wilson, S. H.; Kraut, J. *Science* **1994**, *264*, 1891.
- (73) Sawaya, M. R.; Prasad, R.; Wilson, S. H.; Kraut, J.; Pelletier, H. *Biochemistry* **1997**, *36*, 11205.
- (74) Kamtekar, S.; Berman, A. J.; Wang, J.; Lazaro, J. M.; de Vega, M.; Blanco, L.; Sala, M.; Steitz, T. A. *Mol. Cell* **2004**, *16*, 609.
- (75) Yang, G.; Franklin, M.; Li, J.; Lin, T. C.; Konigsberg, W. *Biochemistry* **2002**, *41*, 2526.
- (76) Rodriguez, A. C.; Park, H. W.; Mao, C.; Beese, L. S. *J. Mol. Biol.* **2000**, *299*, 447.
- (77) Hopfner, K. P.; Eichinger, A.; Engh, R. A.; Laue, F.; Ankenbauer, W.; Huber, R.; Angerer, B. *Proc. Natl. Acad. Sci. U.S.A.* **1999**, *96*, 3600.
- (78) Zhao, Y.; Jeruzalmi, D.; Moarefi, I.; Leighton, L.; Lasken, R.; Kuriyan, J. *Structure* **1999**, *7*, 1189.
- (79) Huang, H.; Chopra, R.; Verdine, G. L.; Harrison, S. C. *Science* **1998**, *282*, 1669.
- (80) Kohlstaedt, L. A.; Wang, J.; Friedman, J. M.; Rice, P. A.; Steitz, T. A. *Science* **1992**, *256*, 1783.
- (81) Jacobo-Molina, A.; Clark, A. D., Jr.; Williams, R. L.; Nanni, R. G.; Clark, P.; Ferris, A. L.; Hughes, S. H.; Arnold, E. *Proc. Natl. Acad. Sci. U.S.A.* **1991**, *88*, 10895.
- (82) Kiefer, J. R.; Mao, C.; Braman, J. C.; Beese, L. S. *Nature* **1998**, *391*, 304.

- (83) Johnson, S. J.; Taylor, J. S.; Beese, L. S. *Proc. Natl. Acad. Sci. U.S.A.* **2003**, *100*, 3895.
- (84) Richartz, A.; Höltje, M.; Brandt, B.; Schäfer-Korting, M.; Höltje, H. D. *J. Enzyme Inhib. Med. Chem.* **2008**, *23*, 94.
- (85) Kuroita, T.; Matsumura, H.; Yokota, N.; Kitabayashi, M.; Hashimoto, H.; Inoue, T.; Imanaka, T.; Kai, Y. *J. Mol. Biol.* **2005**, *351*, 291.
- (86) Firbank, S. J.; Wardle, J.; Heslop, P.; Lewis, R. J.; Connolly, B. A. *J. Mol. Biol.* **2008**, *381*, 529.
- (87) Beard, W. A.; Osheroff, W. P.; Prasad, R.; Sawaya, M. R.; Jaju, M.; Wood, T. G.; Kraut, J.; Kunkel, T. A.; Wilson, S. H. *J. Biol. Chem.* **1996**, *271*, 12141.
- (88) Pelletier, H.; Sawaya, M. R.; Wolfle, W.; Wilson, S. H.; Kraut, J. *Biochemistry* **1996**, *35*, 12742.
- (89) Wong, J. H.; Fiala, K. A.; Suo, Z.; Ling, H. *J. Mol. Biol.* **2008**, *379*, 317.
- (90) Götte, M. *Curr. Pharm. Des.* **2006**, *12*, 1867.
- (91) Boyer, P. L.; Sarafianos, S. G.; Arnold, E.; Hughes, S. H. *J. Virol.* **2001**, *75*, 4832.
- (92) Reverse transcriptase inhibitors designated as nucleoside analogues lack the 3'-OH group on the deoxyribose moiety that is required for subsequent primer elongation and, thus, makes them chain-terminators.
- (93) Naeger, L. K.; Margot, N. A.; Miller, M. D. *Antiviral Ther.* **2001**, *6*, 115.
- (94) Mizrahi, V.; Benkovic, P.; Benkovic, S. J. *Proc. Natl. Acad. Sci. U.S.A.* **1986**, *83*, 5769.
- (95) Dahlberg, M. E.; Benkovic, S. J. *Biochemistry* **1991**, *30*, 4835.
- (96) Petruska, J.; Sowers, L. C.; Goodman, M. F. *Proc. Natl. Acad. Sci. U.S.A.* **1986**, *83*, 1559.
- (97) Devadoss, B.; Lee, I.; Berdis, A. J. *Biochemistry* **2007**, *46*, 4486.
- (98) Reha-Krantz, L. J.; Stocki, S.; Nonay, R. L.; Dimayuga, E.; Goodrich, L. D.; Konigsberg, W. H.; Spicer, E. K. *Proc. Natl. Acad. Sci. U.S.A.* **1991**, *88*, 2417.
- (99) Kuchta, R. D.; Benkovic, P.; Benkovic, S. J. *Biochemistry* **1988**, *27*, 6716.
- (100) Reineks, E. Z.; Berdis, A. J. *J. Mol. Biol.* **2003**, *328*, 1027.
- (101) Carroll, S. S.; Benkovic, S. J. *Chem. Rev.* **1990**, *90*, 1291.
- (102) Kroutil, L. C.; Frey, M. W.; Kaboord, B. F.; Kunkel, T. A.; Benkovic, S. J. *J. Mol. Biol.* **1998**, *278*, 135.
- (103) Woodside, A. M.; Guengerich, F. P. *Biochemistry* **2002**, *41*, 1039.
- (104) Reha-Krantz, L. J.; Bessman, M. J. *J. Mol. Biol.* **1981**, *145*, 677.
- (105) Santos, M. E.; Drake, J. W. *Genetics* **1994**, *138*, 553.
- (106) Reha-Krantz, L. J. *Genetics* **1998**, *148*, 1551.
- (107) Wang, C. X.; Zakharova, E.; Li, J.; Joyce, C. M.; Wang, J.; Konigsberg, W. *Biochemistry* **2004**, *43*, 3853.
- (108) Elisseeva, E.; Mandal, S. S.; Reha-Krantz, L. J. *J. Biol. Chem.* **1999**, *274*, 25151.
- (109) Baker, R. P.; Reha-Krantz, L. J. *Proc. Natl. Acad. Sci. U.S.A.* **1998**, *95*, 3507.
- (110) McCormick, J. E.; McElhinney, R. S. *Eur. J. Cancer* **1990**, *26*, 207.
- (111) Havelka, A. M.; Berndtsson, M.; Olofsson, M. H.; Shoshan, M. C.; Linder, S. *Mini Rev. Med. Chem.* **2007**, *7*, 1035.
- (112) Hoffmann, G. R. *Mutat. Res.* **1980**, *75*, 63.
- (113) Marchesi, F.; Turriziani, M.; Tortorelli, G.; Avvisati, G.; Torino, F.; De Vecchis, L. *Pharmacol. Res.* **2007**, *56*, 275.
- (114) McCarroll, N.; Keshava, N.; Cimino, M.; Chu, M.; Dearfield, K.; Keshava, C.; Kligerman, A.; Owen, R.; Protzel, A.; Putzrath, R.; Schoeny, R. *Environ. Mol. Mutagen.* **2008**, *49*, 117.
- (115) Spratt, T. E.; Levy, D. E. *Nucleic Acids Res.* **1997**, *25*, 3354.
- (116) Reha-Krantz, L. J.; Nonay, R. L.; Day, R. S.; Wilson, S. H. *J. Biol. Chem.* **1996**, *271*, 20088.
- (117) Khare, V.; Eckert, K. A. *J. Biol. Chem.* **2001**, *276*, 24286.
- (118) Lindahl, T. *Mutat. Res.* **1990**, *238*, 305.
- (119) Sanderson, B. J.; Shield, A. J. *Mutat. Res.* **1996**, *355*, 41.
- (120) Dodson, M. L.; Lloyd, R. S. *Free Radical Biol. Med.* **2002**, *32*, 678.
- (121) Sung, J. S.; Demple, B. *FEBS J.* **2006**, *273*, 1620.
- (122) Mozzherin, D. J.; Shibutani, S.; Tan, C. K.; Downey, K. M.; Fisher, P. A. *Proc. Natl. Acad. Sci. U.S.A.* **1997**, *94*, 6126.
- (123) Sheriff, A.; Motea, E.; Lee, I.; Berdis, A. J. *Biochemistry* **2008**, *47*, 8527.
- (124) Berdis, A. J. *Biochemistry* **2001**, *40*, 7180.
- (125) Strauss, B. S. *Bioessays* **1991**, *13*, 79.
- (126) Devadoss, B.; Lee, I.; Berdis, A. J. *Biochemistry* **2007**, *46*, 13752.
- (127) Lee, I.; Berdis, A. *ChemBioChem* **2006**, *7*, 1990.
- (128) Hays, H.; Berdis, A. J. *Biochemistry* **2002**, *41*, 4771.
- (129) Randerath, K.; Randerath, E.; Zhou, G. D.; Li, D. *Mutat. Res.* **1999**, *424*, 183.
- (130) Reardon, J. T.; Sancar, A. *Prog. Nucleic Acid Res. Mol. Biol.* **2005**, *79*, 183–235.
- (131) Gibbs, P. E.; McDonald, J.; Woodgate, R.; Lawrence, C. W. *Genetics* **2005**, *169*, 575.
- (132) Smith, C. A.; Baeten, J.; Taylor, J. S. *J. Biol. Chem.* **1998**, *273*, 21933.
- (133) Tissier, A.; Frank, E. G.; McDonald, J. P.; Iwai, S.; Hanaoka, F.; Woodgate, R. *EMBO J.* **2000**, *19*, 5259.
- (134) O'Neil, L. L.; Grossfield, A.; Wiest, O. *J. Phys. Chem. B* **2007**, *111*, 11843.
- (135) Li, Y.; Dutta, S.; Double, S.; Bdur, H. M.; Taylor, J. S.; Ellenberger, T. *Nat. Struct. Mol. Biol.* **2004**, *11*, 784.
- (136) Sun, L.; Wang, M.; Kool, E. T.; Taylor, J. S. *Biochemistry* **2000**, *39*, 14603.
- (137) Devadoss, B.; Lee, I.; Berdis, A. J. *Biochemistry* **2007**, *46*, 4486.
- (138) Suo, Z.; Lippard, S. J.; Johnson, K. A. *Biochemistry* **1999**, *38*, 715.
- (139) Jacobo-Molina, A.; Arnold, E. *Biochemistry* **1991**, *30*, 6351.
- (140) Choi, J. H.; Besaratinia, A.; Lee, D. H.; Lee, C. S.; Pfeifer, G. P. *Mutat. Res.* **2006**, *599*, 58–65.
- (141) Washington, M. T.; Minko, I. G.; Johnson, R. E.; Haracska, L.; Harris, T. M.; Lloyd, R. S.; Prakash, S.; Prakash, L. *Mol. Cell. Biol.* **2004**, *24*, 6900.
- (142) Shcherbakova, P. V.; Fijalkowska, I. J. *Front. Biosci.* **2006**, *11*, 2496.
- (143) Servant, L.; Bieth, A.; Hayakawa, H.; Cazaux, C.; Hoffmann, J. S. *J. Mol. Biol.* **2002**, *315*, 1039.
- (144) Lin, Q.; Clark, A. B.; McCulloch, S. D.; Yuan, T.; Bronson, R. T.; Kunkel, T. A.; Kucherlapati, R. *Cancer Res.* **2006**, *66*, 87.
- (145) Pagès, V.; Johnson, R. E.; Prakash, L.; Prakash, S. *Proc. Natl. Acad. Sci. U.S.A.* **2008**, *105*, 1170.
- (146) Nair, D. T.; Johnson, R. E.; Prakash, L.; Prakash, S.; Aggarwal, A. K. *Science* **2005**, *309*, 2219.
- (147) Cleaver, J. E. *J. Dermatol. Sci.* **2000**, *23*, 1.
- (148) Stary, A.; Kannouche, P.; Lehmann, A. R.; Sarasin, A. *J. Biol. Chem.* **2003**, *278*, 18767.
- (149) Sun, L.; Zhang, K.; Zhou, L.; Hohler, P.; Kool, E. T.; Yuan, F.; Wang, Z.; Taylor, J. S. *Biochemistry* **2003**, *42*, 9431.
- (150) Ling, H.; Boudsocq, F.; Plosky, B. S.; Woodgate, R.; Yang, W. *Nature* **2003**, *424*, 1083.
- (151) Vaisman, A.; Masutani, C.; Hanaoka, F.; Chaney, S. G. *Biochemistry* **2000**, *39*, 4575.
- (152) Alt, A.; Lammens, K.; Chiochini, C.; Lammens, A.; Pieck, J. C.; Kuch, D.; Hopfner, K. P.; Carell, T. *Science* **2007**, *318*, 967.
- (153) Chen, Y. W.; Cleaver, J. E.; Hanaoka, F.; Chang, C. F.; Chou, K. M. *Mol. Cancer Res.* **2006**, *4*, 257–265.
- (154) Albertella, M. R.; Green, C. M.; Lehmann, A. R.; O'Connor, M. J. *Cancer Res.* **2005**, *65*, 9799.
- (155) Berdis, A. J. *Biochemistry* **2008**, *47*, 8253.
- (156) Kerr, S. G.; Anderson, K. S. *Biochemistry* **1997**, *36*, 14064.
- (157) Yang, G.; Wang, J.; Cheng, Y.; Dutschman, G. E.; Tanaka, H.; Baba, M.; Cheng, Y. C. *Antimicrob. Agents Chemother.* **2008**, *52*, 2035.
- (158) Gu, Z.; Arts, E. J.; Parniak, M. A.; Wainberg, M. A. *Proc. Natl. Acad. Sci. U.S.A.* **1995**, *92*, 2760.
- (159) Anderson, V. R.; Perry, C. M. *Drugs* **2007**, *67*, 1633.
- (160) Gandhi, V.; Plunkett, W. *Clin. Pharmacokinet.* **2002**, *41*, 93.

CR800530B